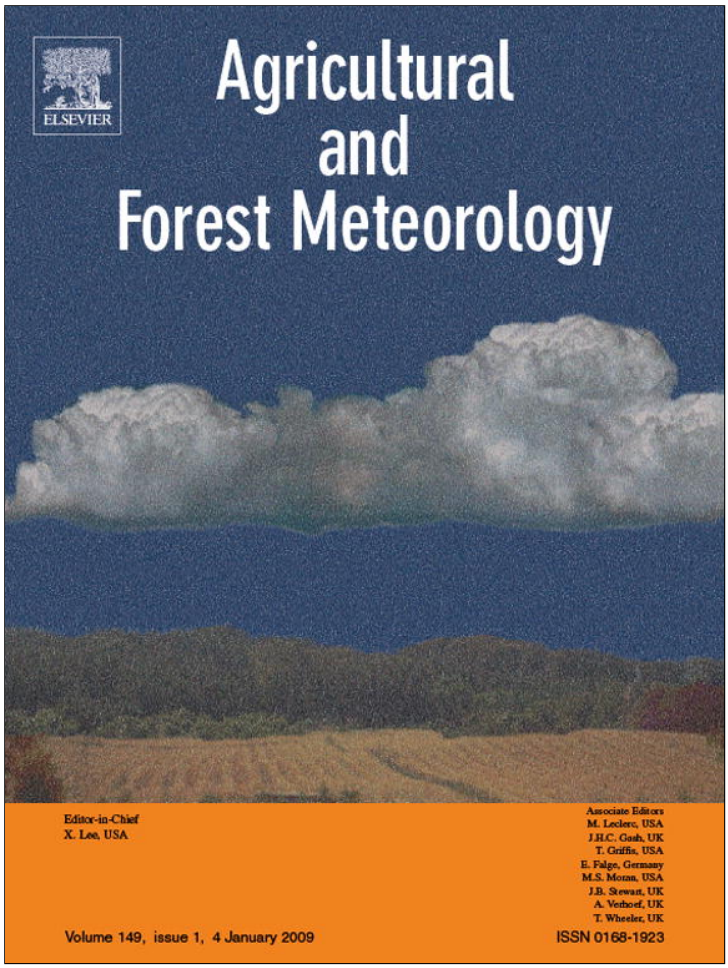

available at www.sciencedirect.com

ScienceDirect

journal homepage: www.elsevier.com/locate/agrformet

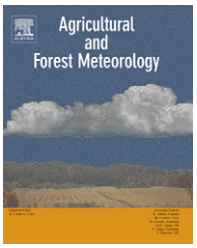

Canopy dynamics and phenology of a boreal black spruce wildfire chronosequence

Shawn P. Serbin [a,*], *Stith T. Gower* [a], *Douglas E. Ahl* [a,b]

[a] *Department of Forest Ecology and Management, 1630 Linden Drive, University of Wisconsin, Madison, WI 53706, USA*
[b] *Ascend Analytics, 2737 Mapleton Ave, Suite 103, Boulder, CO 80304, USA*

ARTICLE INFO

Article history:
Received 22 August 2007
Received in revised form
19 July 2008
Accepted 7 August 2008

Keywords:
Phenology
Leaf area index (LAI)
Boreal forest
Understory
LAI-2000
F_{IPAR}

ABSTRACT

This research quantified the canopy phenology, growing season and inter-annual dynamics of the overstory and understory vegetation in a boreal wildfire chronosequence in northern Manitoba, Canada. Optical measurements of the canopy radiation regime were made in the 2004–2006 growing seasons to evaluate the spatial and temporal variation in the effective leaf area index (L_e) and fraction of intercepted photosynthetic active radiation (F_{IPAR}) of the canopy.

Black spruce dominated the overstory L_e (L_e^O) in the oldest stands (74- and 154-year-old), while deciduous shrub and tree species dominated the youngest stands (1- to 23-year-old). L_e^O varied from a minimum (mean ± S.D.) of 0.26 ± 0.33 to a maximum of 2.33 ± 1.20 and from 0.63 ± 0.56 to 1.20 ± 0.56 for the understory vegetation (L_e^U). F_{IPAR}^O was negligible in the youngest stands, and reached a peak in the oldest stands studied. L_e^U comprised a significant percentage of total L_e (>30%) and F_{IPAR} (>20%) for all stands, except the oldest, 154-year-old stand.

We observed two key features in the L_e and F_{IPAR} seasonal cycles: (i) significant changes ($p < 0.001$) in L_e^U, increasing by 41% across all sites; and (ii) >80% difference in seasonality exhibited by the overstory in the mixed/deciduous and black spruce dominated stands. L_e varied by less than 20% among the three years. Canopy green-up was positively correlated to spring temperatures and occurred within 20–28 days for all stands. The pronounced increase in wildfires in the boreal forest in recent years necessitates additional studies to better understand their effects on the species composition and structure of canopies of all vegetation strata.

1. Introduction

The boreal forest is the second largest forested biome (Gower et al., 2001) and comprises nearly 30% of the Earth's total forested area (Conard et al., 2002). The vast area of the boreal forest makes it important to the terrestrial carbon, water and energy cycles, as evidenced by the influence of the seasonal carbon dynamics of boreal forests on seasonal global atmospheric CO_2 concentrations (e.g. D'Arrigo et al., 1987; Bonan, 1991). Atmospheric inversion modeling and inventory-based analyses suggest that high-latitude ecosystems are currently a net carbon sink (e.g. Tans et al., 1990; Ciais et al., 1995; Goodale et al., 2002), but the general location of the carbon sink and its seasonal strength are still debated (e.g. Buermann et al., 2007; Stephens et al., 2007).

The role of the boreal forest in the global carbon cycle may be affected by climate change (e.g. Wu and Lynch, 2000; Potter, 2004; Notaro et al., 2007). There is considerable evidence that

* *Corresponding author*. Tel.: +1 608 262 6369.
E-mail addresses: serbin@wisc.edu, serbinsh@gmail.com (S.P. Serbin).
0168-1923/$ – see front matter
doi:10.1016/j.agrformet.2008.08.001

warming is underway in the North American boreal region—particularly in the winter and spring (Chapman and Walsh, 1993; Lucht et al., 2002). Predicted warming may impact boreal forest canopy dynamics, such as the leaf area index (LAI), fraction of intercepted photosynthetic active radiation (F_{IPAR}) by the vegetation, and canopy phenology, which are all key drivers in carbon uptake (Bonan, 1993; White et al., 1997; Running et al., 2004). The variation of vegetation phenology to short- and long-term climate variability is an important indicator of changes to the biosphere (Penuelas and Filella, 2001; Badeck et al., 2004) and the timing of phenological stages of boreal vegetation (i.e. LAI and F_{PAR}) directly influence seasonal CO_2 assimilation and radiation balance (Barr et al., 2004; Amiro et al., 2006).

Early warm and wet spring conditions in the boreal forests increase early season photosynthetic activity (e.g. Goulden et al., 1998; Black et al., 2000; Chen et al., 2006a) and lengthen the growing season (Beaubien and Freeland, 2000). Analysis of historic Advanced Very High Resolution Radiometer (AVHRR) satellite data led scientists to suggest that warmer temperatures caused earlier canopy green-up and photosynthetic activity over the last two decades in the mid- to high-latitude biomes, including the boreal forest (e.g. Myneni et al., 1997; Slayback et al., 2003; Zhou et al., 2003). The exact mechanisms for such increases, however, remain largely uncertain due to the large spatial and temporal variation in vegetation response to climate changes (Keeling et al., 1996; Bogaert et al., 2002). However, stress-induced factors, possibly mid-season drought, reduced peak vegetation greenness and photosynthetic uptake for the continental boreal region (e.g. Angert et al., 2005; Bunn et al., 2005; Goetz et al., 2005). Further analyses, coupled to ground measurements, are needed to resolve these contradictory results. This is especially true for North American boreal forests that are experiencing increased large, stand replacing wildfires that alter the composition and structure of vegetation surface characteristics (Liu et al., 2005; Amiro et al., 2006). In addition, the combined impacts of fire and insect outbreaks on inter-annual variations in the carbon cycle of Canadian boreal forests can be large for particular years (Kurz and Apps, 1999) and may increase with continued climate change (Kurz et al., 2008). These large-scale changes in vegetation may confound the response of boreal vegetation to climate change.

Climate warming may increase the occurrence of extensive and severe wildfires in boreal forests (Stocks et al., 1998; Flannigan et al., 2005), with select years responsible for CO_2 emissions that are significant contributors to annual global budget (e.g. Kurz and Apps, 1999; Amiro et al., 2001; van der Werf et al., 2006). Increased fire frequency shortens the recovery period between fires and exacerbates carbon releases from boreal forest through combustion (Kasischke et al., 1995; Bond-Lamberty et al., 2007). Stand-killing wildfires reset forest succession and thus influence vegetation composition and canopy structure (Van Cleve et al., 1986; Bond-Lamberty et al., 2002; Greene et al., 2004). For example, in northern Manitoba, deciduous plants are common pioneer species and persist in the overstory for 30–60 years on well-drained soils and are replaced by evergreen conifers during stand succession in many North American boreal regions (Bond-Lamberty et al., 2004; Martin and Gower, 2006). However this successional pathway can be altered by an increased fire return interval (Johnstone, 2006; Johnstone and Chapin, 2006b). Edaphic conditions can also influence species composition. This natural successional process can change canopy structure, functioning and phenology because the inherent differences of the characteristics between evergreen and deciduous species.

The overall objective of this research was to quantify the seasonal variation in growing season canopy phenology of the overstory and understory vegetation, for a well- and poorly-drained boreal forest wildfire chronosequence. Specific objectives were (1) quantify and compare the LAI and F_{IPAR} of overstory and understory vegetation for a well- and poorly-drained boreal forest wildfire chronosequence, (2) quantify the growing season and inter-annual variation in canopy phenology for the chronosequences, and (3) examine the variation in LAI and F_{IPAR} for the boreal landscape comprised of well- and poorly-drained stands.

We hypothesized that (1) optical sensors will effectively characterize the seasonality and variation in LAI and F_{IPAR} in the early successional stands, but will not adequately characterize the small seasonal changes in needle leaf area of conifer dominated stands, as these trees retain needles for 10–20 years; (2) canopy green-up will occur earlier in young deciduous stands and later in black spruce stands; and (3) the variability of LAI and F_{PAR} in young stands will be high compared to older, conifer dominated stands due to the patterns of vegetation re-growth.

2. Study area and methodology

Field measurements were conducted near Thompson, Manitoba, Canada, from 2004 to 2006. Wildfire is a natural part of the ecology of the boreal forests in this region. The experimental design of this study includes a wildfire chronosequence comprised of stands that originated from stand-replacing wildfires that occurred in 1850, 1930, 1964, 1981, 1989, 1994 and 2003. This region was part of the Boreal Ecosystem and Atmospheric Study (BOREAS)—Northern Study Area (55°53′N, 98°20′W), and is a NASA Earth Observing System (EOS) core validation site (http://landval.gsfc.nasa.gov/). Elevation ranges from about 178 to 350 m above sea level. The mean annual temperatures were 1.64, 0.44, and −0.81 °C for 2004, 2005, and 2006, respectively. Mean air temperatures for January and July for the three years of study were −24 and 18 °C, respectively. Annual precipitation averaged 604 mm (±263.8 mm).

2.1. Study sites

All burn sites were within a 40-km^2 area, except for the 1994 burn, which was located approximately 80-km northeast from the other stands. Excluding the 1994 burn, all these sites were part of the boreal forest wildfire chronosequence study (Wang et al., 2003; Bond-Lamberty et al., 2004). At the beginning of the study, sites ranged in age from approximately 1- to 154-years-old (Bond-Lamberty et al., 2004, Serbin, unpublished data). The stands encompassed the natural range of ages, basal area, density, and canopy closure of boreal forests in this region (Table 1).

Table 1 – Overstory stand structural characteristics for the chronosequence sites, by soil drainage (i.e. well- and poorly-drained) and stand age

Stand characteristics	Years since last major fire (burn year)						
	1 (2003)	10 (1994)	15 (1989)	23 (1981)	40 (1964)	74 (1930)	154 (1850)
Well-drained stands							
Measurement plots	11	18	17	18	16	16	16
Tree diameter	0.0 (–)	5.7 (3.6)	5.2 (3.4)	8.3 (6.1)	10.0 (5.8)	9.9 (3.1)	11.3 (3.2)
Basal area (m^2 ha^{-1})	0.0 (–)	1.6 (0.2)	1.6 (0.2)	12.2 (1.2)	9.2 (1.1)	18.5 (5.3)	25.0 (6.1)
Density (Trees ha^{-1})	0.0 (–)	1025 (116)	2676 (178.6)	5622 (411)	3534 (384.9)	3936 (135.3)	4991 (169.4)
% black spruce	0.0	1.5	2.0	4.0	40.0	88.0	96.0
Poorly-drained stands							
Measurement plots	11	13	12	12	16	14	14
Tree diameter	0.0 (–)	0.0 (–)	2.9 (4.2)	7.5 (6.0)	7.2 (5.0)	8.5 (2.6)	7.2 (1.8)
Basal area (m^2 ha^{-1})	0.0 (–)	0.0 (–)	0.3 (0.1)	1.9 (0.3)	4.6 (0.5)	7.1 (6.1)	4.5 (6.5)
Density (Trees ha^{-1})	0.0 (–)	0.0 (–)	68.0 (11.0)	253 (47.6)	3177 (237.5)	2974 (170.0)	4255 (312.5)
% black spruce	0.0	0.5	2.5	14.0	51.0	92.0	98.0

The percent black spruce represents the percentage the total basal area comprised of black spruce within each stand. Elevation data are derived from the Shuttle Radar Topography Mission (SRTM) data available on the EOS Land Validation site (http://landval.gsfc.nasa.gov/).

Common overstory species were black spruce (*Picea mariana*, Michx.), jack pine (*Pinus banksiana*), trembling aspen (*Populus tremuloides*) and willow (*Salix* spp.); other less common tree species included paper birch (*Betula papyrifera*, Marsh.), tamarack (*Larix laricina*, (Du Roi) Koch.) and balsam poplar (*Populus balsamifera*, L.). Early successional sites (1994–1989) were largely dominated by willow, jack pine, and aspen in the overstory, with fireweed (*Epilobium angustifolium*, L.), wild rose, Labrador tea and blueberry (*Vaccinium myrtilloides*, Michx) in the understory. The youngest site (2003) contained mostly herbaceous understory species such as wild rose, fireweed, and horsetail (*Equisetum* spp.) with Labrador tea, willow and periodic black spruce seedlings also present. Mid-successional sites (1981–1964) were dominated by a mix of the deciduous and coniferous species in the overstory, with an understory of cranberry (*Vaccinium vitisidaea*), bearberry (*Arctostaphylos uva ursi*, L.), Labrador tea and bog birch. The oldest stands (1930 and 1850) were dominated by black spruce, with a few jack pine, aspen, balsam poplar and tamarack, with an understory shrub layer of Labrador tea, willow, and green alder (*Alnus crispa*, (Alt.) Pursch) and herbaceous vegetation. These sites were selected to minimize differences in site and stand history factors such as soil, topography and wildfire history (Bond-Lamberty et al., 2004; Goulden et al., 2006).

Our notation for the presentation of results follows Bond-Lamberty et al. (2002) who used ''site'' to describe a forest patch by year of the most recent stand-killing fire (i.e. 1994 and 1989) and ''stand'' refers to the drainage condition within a site (i.e. well-drained or poorly-drained). Poorly-drained refers to forest stands located in topographic depressions that have sphagnum mosses (*Sphagnum* spp.) as the dominant bryophytes, a high water table, often with standing water, and a thicker peat layer with root growth occurring below the water table (Bisbee et al., 2001). Well-drained stands typically have feather mosses (usually *Pleurozium, ptilium, Hylocomium* spp.) as the dominant bryophyte species and reindeer lichen (*Cladina* spp.), occur on upland topographic features, with roots growing above a deeper water table and a shallower peat layer (Bisbee et al., 2001). This study is also part of a larger study to validate MODerate resolution Imaging Spectroradiometer (MODIS) vegetation products for the boreal landscape; we therefore present site-level, or landscape-level, averages which are arithmetic mean of both the well- and poorly-drained stands for a site which present the landscape scale variation in LAI and F_{PAR} viewed by a moderate resolution sensor.

2.2. Field sampling design

The sampling design followed protocols of validation of moderate-resolution satellite data products (Morisette et al., 2006). At each site, two parallel 2 km transects, separated by 100 m were established to characterize the spatial vegetation pattern for each burn of a uniform age. Individual plots were equally spaced 150 m apart, for a total of 30 plots per burn site. The size and layout of plots along transects followed Burrows et al. (2002). Spatial variability of the land-cover was quantified using a variogram analysis of satellite reflectance data at differing resolutions (i.e. Landsat, ASTER and MODIS). We used 15–250 m normalized difference vegetation index (NDVI) data as our state variables and the proxy for determining spatial heterogeneity of the vegetation canopy architecture (Tian et al., 2002; Tarnavsky et al., 2008). These data, in combination with satellite derived information on the seasonal variation of the vegetation, allowed us to efficiently sample the vegetation by locating plots within relatively homogenous areas of vegetation cover that matched the overall seasonal signal of the entire burn area.

Transects contain up to a pair of MODIS 1 × 1 km pixels per site and several 250 m surface reflectance pixels. The upper limit of the number of plots was strongly influenced by logistics for field sampling in the remote region dissected by wetlands. The location of the center (±6–20 m) for each ground plot was determined in the field with hand-held global positioning system (GPS) receivers (Garmin e-Trex Vista, Olathe, Kansas) in the spring of 2004, prior to initial leaf expansion.

2.3. Field data collection

Measurements of the canopy radiation regime were collected at key phenological periods (i.e. leaf-off, green-up, peak LAI, and onset of senescence) in the 2004, 2005, and 2006 growing seasons. F_{IPAR} is provided as a surrogate of the canopy F_{PAR}, as these values are similar for most conditions (Gower et al., 1999; Gobron et al., 2006). F_{IPAR} vegetation phenology (i.e. changes in canopy light interception with increased seasonal foliage development) was measured for a limited time period in the 2004 growing season and continuously throughout the 2005 and 2006 growing seasons. Stand structural characteristics of the overstory (i.e. basal area, species composition, tree density, etc.) were measured at the center of each 30 plot at each site in 2005–2006 using 1–2 $m^2\,ha^{-1}$ basal area factor (BAF) prisms and variable-radius subplots.

2.4. Optical measurements of LAI and F_{IPAR}

Optical measurements of effective LAI (L_e) and F_{IPAR} were collected using the LAI-2000 Plant Canopy Analyzer (PCA; Li-Cor BioSciences, Lincoln, Nebraska). The LAI-2000 measures the canopy gap fraction simultaneously across five zenith angles or annuli (0–75°) from the transmission of diffuse blue-sky radiation ($\lambda < 490$ nm) through the canopy, by means of a fisheye lens to projecting a nearly hemispherical view of the canopy onto the sensor (Welles and Norman, 1991). The optical filter minimizes the scattering of radiation from the canopy (Li-Cor, 1991). The L_e, or plant area index, includes radiation interception by all elements in the canopy, including leaves and woody non-photosynthetic tissues and assumes a random (spherical) spatial distribution of foliage elements (Chen and Black, 1992; Gower et al., 1999). F_{IPAR} is derived from the integrated transmission of radiation (i.e. over all annuli) through the canopy elements or as $F_{IPAR} = 1 - \tau$. The LAI-2000 PCA requires uniform diffuse sky to acquire the highest quality data. We restricted our data collection to dawn and dusk (when the sun was hidden by the horizon) or when the sky was uniformly overcast to avoid direct beam radiation.

The optical measurements of the vegetation were designed to quantify the radiation regime for the overstory (L_e^O and F_{IPAR}^O) and understory (L_e^U and F_{IPAR}^U). The overstory was quantified using measurements over the understory layer, or about 1 m above the ground, while the total canopy (L_e^T and F_{IPAR}^T) vegetation was measured just above the soil or moss surface. L_e^U and F_{IPAR}^U were calculated as the difference between the total and overstory canopy measurements.

To provide comparison of our optical results with previously reported LAI values across stand types within the Canadian boreal region (e.g. Chen et al., 1997b; Leblanc and Chen, 2001; Chen et al., 2006b) we provide maximum growing season overstory LAI for the conifer (LAI_C) and deciduous stands (LAI_D), using Eqs. (1) and (2), respectively.

$$LAI_C = \frac{(1-\alpha)L_e\gamma_E}{\Omega_E} \quad (1)$$

$$LAI_D = \frac{L_e}{\Omega} - \alpha \quad (2)$$

where L_e is the effective LAI, γ_E the needle-to-shoot area ratio, Ω_E the elemental clumping index and α is the woody-to-total leaf area ratio ($\alpha = W/L_e(\gamma_E/\Omega_E)$, where W represents the woody-surface-area-index (half the woody area m^{-2} ground area)). We used values of γ_E, α, Ω_E for boreal tree species from the literature (e.g. Chen and Cihlar, 1995; Chen et al., 1997b; Gower et al., 1999) which were weighted accordingly, by the tree basal area within measurement plots, and estimated α using averaged leaf-off LAI-2000 data.

The LAI-2000 sample dates spanned the range of growing season phenology from leaf-off through the onset of canopy senescence, visually defined by the stage of leaf development; leaf-off: no foliage on deciduous trees, buds may be present and no green understory; green-up: period of canopy development by deciduous species; canopy maturity: canopy and understory canopy complete or stable; onset of canopy senescence: beginning of leaf coloring and reduction in understory biomass. Each plot mean was based on a LAI-2000 measurement at plot center and 10 m from center in the four cardinal directions for a total of five overstory and five total canopy measurements. A reference LAI-2000 PCA was setup on top of a nearby tower, above the canopy, and programmed to collect data every 15 s. Reference and field measurements with the instruments were taken simultaneously and all LAI-2000 units were inter-calibrated at least once a season.

We also investigated the effects of multiple scattering, or contamination of the optical measurements on the computed L_e, left after accounting for diffuse sky conditions (Leblanc and Chen, 2001; Chen et al., 2006b). Using sensitivity analysis we concluded the optimal ring selection included all but the lowest zenith angles (i.e. fifth annuli). The inclusion of all rings in the calculation of L_e resulted in a systematic 14% reduction in L_e, and the retrievals based on the first four rings were highly consistent ($L_e^4 = 1.01 \times L_e^{1-4}$, $R^2 = 0.99$) with reference retrievals, based on ring four alone (Leblanc and Chen, 2001). Therefore, all data reported in this study are based on the first four rings.

2.5. Automated measurements of radiation interception

Automated continuous measurements of incident and F_{IPAR} were made with LI-191SA Line Quantum Sensors (Li-Cor BioSciences, Lincoln, Nebraska). At each site, up to four line quantum sensors were positioned in four cardinal directions below the canopy at maximum cable length (32 m), and one sensor was mounted on the tower above the canopy. The below canopy LI-191SA sensors were installed on metal stakes to ensure each sensor was level and above the ground to avoid damage from surface moisture. The sensors were deployed in each stand in early spring (~DOY 110) to capture the seasonal dynamics of canopy light interception for canopy foliage, and maintained through the growing season. The logistics of getting all the sites established in the spring of 2004 prevented us from measuring early growing season canopy dynamics for all the sites. Sensors were removed in October (~DOY 295) prior to major snowfall.

Minimum and maximum values for transmitted PAR measured with each sensor were recorded every 10 s and output as hourly averages using a data logger at each site

(Campbell Scientific, Logan Utah). The data were post-processed to remove erroneous values due to weather conditions and data interruptions or values including the following criteria:

(i) PAR_{above} (incident PAR) < PAR_{below} (PAR below the canopy) and,
(ii) $PAR_{below} < 0$.

After filtering poor quality data, we calculated daily integrated F_{IPAR}. We filled gaps in incident PAR data using the modeled relationships between individual sites above canopy sensors. The distance between towers was generally less than 20 km. We did not fill missing values in the below canopy measurements as the majority of missing data were less than 15 days per site and sufficiently spread throughout the growing season that we had adequate data to model vegetation phenology.

2.6. Determining key canopy phenological transitions

Sigmoid logistic growth models have been used to characterize the temporal trends of canopy phenology across a wide range of vegetation types (e.g. Ahl et al., 2006; Frolking et al., 2006; Fisher et al., 2007; Zhang et al., 2007). This model effectively quantifies the four key transitions that may be remotely sensed with optical data (Zhang et al., 2003): (1) leaf emergence or onset of greenness; (2) maximum biomass or peak LAI and F_{IPAR}; (3) the onset of leaf senescence; and (4) onset of vegetation dormancy by the completion of leaf abscission (Dixon, 1976) and leaf-fall, for deciduous species. Eq. (3) was used to fit the ascending and descending time-series of F_{IPAR} data for each site in the MODEL procedure using SAS (SAS Institute Inc., 2001, Cary, North Carolina) following Zhang et al. (2003):

$$y(t) = \frac{c}{1 + e^{a+bt}} + d \quad (3)$$

where $y(t)$ is the F_{IPAR} value measured with the LI-191SA radiation sensor at time t, a and b are empirically derived coefficients that control the phase and slope, d is an initial background value, and c is the potential maximum value of F_{IPAR}.

We used the curvature change rate (CCR) equation following Zhang et al. (2003) to calculate the phenological transition dates. During green-up, the rate-of-change of curvature of the F_{IPAR} time-series exhibits local maxima surrounding the inflection, or the points of greatest curvature at the base and top of the sigmoid model (Zhang et al., 2003). Similarly, we defined the phenological transitions of onset of senescence and vegetation dormancy as the local minima around the inflections on the descending sigmoid curve. The transition dates determined with the combination of Eq. (3) and the CCR were calculated with a mean, median and a corresponding 95% confidence interval of the mean per site using Monte Carlo simulations in the MODEL procedure.

2.7. Growing-degree-days

We examined the relationship between spring boreal vegetation phenology and air temperature (e.g. Barr et al., 2004), and to a lesser extent, photoperiod (Kramer et al., 2000). We calculated ΣD, or cumulative growing-degree-days (Campbell and Norman, 1998), using a physiologically meaningful base temperature of 0 °C for boreal vegetation (Botta et al., 2000). The ΣD provides a key metric for deriving canopy phenological development stages (e.g. Lechowicz, 1984; Kramer, 1994; Chuine and Cour, 1999; Leinonen and Kramer, 2002) which are useful for parameterizing the dynamic vegetation processes in ecosystem biogeochemical process models that are used to quantify seasonal mass and energy exchanges from vegetation to the atmosphere (Botta et al., 2000). Site-level ΣD was calculated similar to Barr et al. (2004) as

$$\sum D = \sum_{d=d_i}^{d_f} \max(T_a - 0\,^{\circ}\mathrm{C}) \quad (4)$$

where d is the day of year (DOY), d_i and d_f are the initial and final values of d for growing-degree-day calculation. T_a is the mean of the daily maximum and minimum air temperatures, measured at the Northern Old Black Spruce (NOBS) flux tower (Dunn et al., 2007). For the 1994 burn site, we used historical climate data for the nearest weather station (Kelsey Dam, 56°2′N, 96°31′W) that belongs to the Environment Canada historical station network (http://www.climate.weatheroffice.ec.gc.ca/). We identified d_i as the final day of the first three consecutive days where T_a exceeded 0 °C. The value for d_f was defined as the first day after August 1 when T_a was <0 °C. These data were used with the F_{IPAR} data and the phenology models to explore the timing of key spring phenological stages of each site by thermal time (i.e. temperature accumulation requirement). While these data do not provide a definitive thermal requirement for these burn sites, they do portray the relative differences among sites.

2.8. Data analysis

All statistical analyses were conducted using SAS version 9.1.3 software (SAS Institute Inc., 2001). A repeated-measures analysis using the SAS/MIXED procedure was used to evaluate the seasonal changes in L_e (and LAI) and F_{IPAR}, across burn sites and respective years. The year, period of measurement, and all possible interactions were assigned as fixed effects, with the individual plots within a site used as the subject in the repeated measures analysis. Significant differences (at $\alpha = 0.05$) in L_e or F_{IPAR} between successive measurement periods within sites were explored using Tukey's honestly significant differences (HSD) method for all pairwise multiple comparisons of means. We also used linear regression (generalized linear model procedure; GLM) and analysis of variance (ANOVA) to examine the variability of L_e and F_{IPAR} as a function of stand age and soil edaphic conditions. Paired t-tests were used to determine the effects of soil drainage on L_e and F_{IPAR}. Results were used to explore the relationship of canopy structure to species composition and soil edaphic conditions.

Coefficients of variation (CV) were calculated to investigate the plot-to-plot variability in the radiation regime in relation to stand age and soil drainage. Unless otherwise stated all pairwise comparisons and significant differences were evaluated at the $\alpha = 0.05$ significance level.

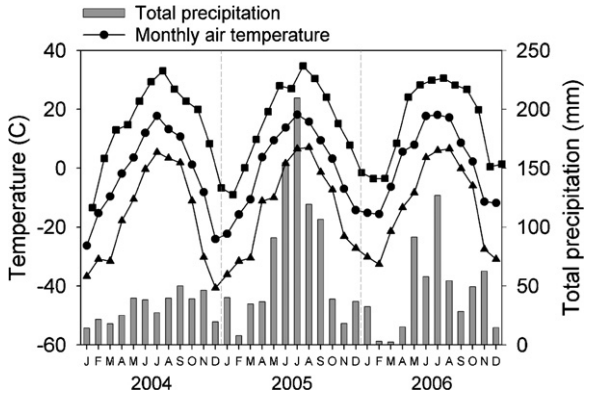

Fig. 1 – Monthly mean air temperature and precipitation for the study area as measured above the canopy (30 m) at the NOBS micrometeorological tower. The filled squares and triangles represent the average monthly maximum and minimum air temperatures, respectively. Note the large increase in precipitation in 2005, particularly from May through September.

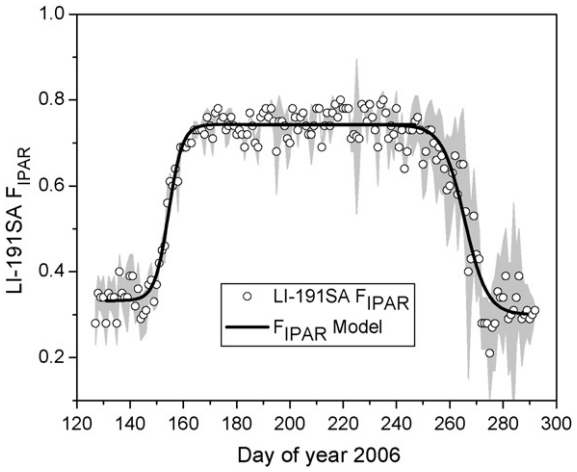

Fig. 2 – Daily F_{IPAR} values from the 1994 burn site for the 2006 growing season. The fitted line represents the modeled phenology trajectory using the daily F_{IPAR} data and fitting Eq. (3), while the shaded region represents the ± one standard deviation of the daily mean values.

3. Results

3.1. *Variations in the overstory stand structure across wildfire chronosequence*

Tree basal area varied significantly across the well- and poorly-drained chronosequences, with a minimum (±1 standard deviation) of $0.57 \pm 0.4\ m^2\ ha^{-1}$ to a maximum of $16.3 \pm 8.4\ m^2\ ha^{-1}$. Within a site, basal area was generally lower in the poorly-drained than well-drained stands (Table 1). Black spruce basal area increased with stand age from negligible values in the 1-year-old stand to a maximum of $15.8 \pm 8.2\ m^2\ ha^{-1}$ in the 154-year-old stand. Average tree diameter increased with stand age to a maximum of 10.7 ± 3.8 in the oldest (74- and 154-year-old) well-drained stands. Tamarack was present in the poorly-drained 40- to 154-year-old stands and averaged 6.3% (1–16%) of the total basal area. The youngest burns (2003 and 1994) also contained standing charred, black spruce snags in the overstory.

3.2. *Continuous F_{IPAR} phenology*

Monthly climatic conditions varied considerably over the three years, with a much cooler and drier spring in 2004 than 2005 and 2006 (Fig. 1). For example, there were 20 more days with $T_a > 0\ ^\circ C$ in 2005 than 2004. Furthermore, total precipitation during the month of July was 63% higher during the 2005 growing season compared to the 2004 and 2006 growing seasons.

The seasonal pattern of foliage development for the primarily deciduous and mixed 40-year-old and younger stands followed a bell-shaped curve during the growing season, closely corresponding to seasonal changes in air temperature and precipitation (Fig. 2). Growing season F_{IPAR} varied from 45% to 60% ($p < 0.0001$) for the 40-year-old and younger stands, while F_{IPAR} varied by a much smaller percentage (6%), but significantly ($p < 0.001$), for the 74- and 154-year-old stands (Fig. 3).

The logistic model simulated canopy F_{IPAR} phenology of the young deciduous stands well, with highly significant fits ($p < 0.0001$ to $p < 0.01$, R^2 between 0.45 and 0.85) to all the spring green-up data. An example of the sigmoid logistic model fit to the daily F_{IPAR} for the 10-year-old burn site is provided in Fig. 2. The model illustrates the rapid increase in F_{IPAR} at the beginning of the growing season.

In general there was a U-shaped relationship between green-up date and day of year for the landscape average of the burn sites (Fig. 4). The mean (±S.D.) day of year (DOY) for canopy green-up for all sites was 148 ± 7.5 and 146 ± 6.0 for the 2005 and 2006 growing seasons, respectively. For the 15- and 40-year-old sites (the only three sites with three years of complete data), onset of greenness occurred on DOY 165 (13th

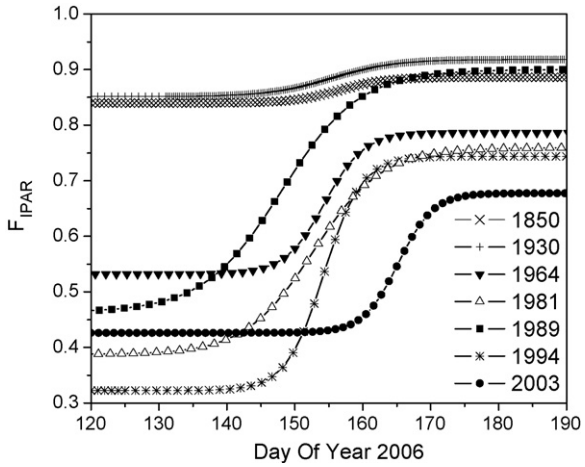

Fig. 3 – Modeled spring phenology for the seven sites comprising the chronosequence fitting Eq. (3) to the daily integrated F_{IPAR} values. Note the distinct differences between the primarily deciduous stands (1981–2003) and coniferous stands (1930 and 1850).

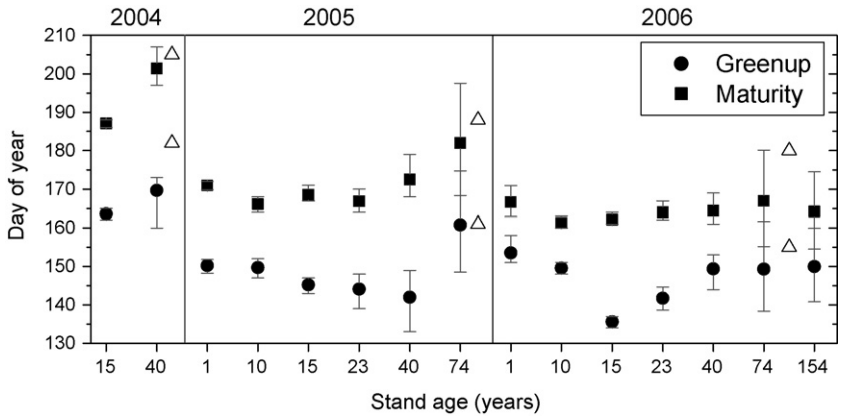

Fig. 4 – Average onset of greenness (filled circles) and maturity (filled squares) calculated with Eq. (3) and the CCR, with the corresponding 95% confidence intervals of the mean derived from the fitting procedure. Data limitations restricted the number of sites displayed for the 2004 and 2005 growing seasons (see text). The open triangles correspond to direct measurements of black spruce bud break and cessation of 95% shoot growth on control trees from a concurrent study at a boreal warming experiment (Bronson et al., under review).

June), 142 (22nd May), and 138 (18th May) for the 2004, 2005, and 2006 growing seasons, respectively, with each year having warmer spring temperatures (Fig. 1). The average length of canopy green-up, the period from green-up onset to canopy maturity, was 22 days. The 15-year-old site (1989 burn) had a significantly ($p < 0.01$) earlier onset of greenness than other sites in 2006. The onset of maturity occurred at a similar day of year for all sites (Fig. 4).

The critical ΣD threshold values by phenological stage (i.e. green-up and maturity) differed dramatically among sites (Table 2). The 15-year-old site had the lowest green-up ΣD (~281 °C days), while the 74-year-old site had the greatest thermal requirement of 503 °C days. Together, the deciduous sites (1 through 23-year-old) had a ~108 day lower ΣD threshold for greenness onset than the coniferous sites (1930 and 1850). The average green-up ΣD for all the sites and years was 400 °C (Table 2). There was generally less variation in the maturity onset ΣD values for individual sites, with an average of 645 and 742 °C days required for the deciduous and conifer sites, respectively. For all the sites measured, the mean onset of senescence for 2004 through 2006 growing seasons occurred on DOY 253 ± 10 (early September) and resulted in an average duration of maximum canopy foliage of 102 days for the deciduous sites.

3.3. *Variation in L_e and F_{IPAR} across the wildfire chronosequence*

Average landscape-level (combined well- and poorly-drained stands) L_e^O increased with stand age, and was 73.6% less in the 15-year-old stand than the two oldest stands dominated by black spruce (Fig. 5). The L_e for the well-drained chronosequence ranged from (mean L_e ($m^2\ m^{-2}$) ± S.E.) 0.34 ± 0.08 for the 1-year-old site to a maximum of 3.13 ± 0.09 for the 74-year-old stands, followed by a significant decline ($p < 0.001$) of 21% in L_e to 2.50 ± 0.08 for the 154-year-old stand. Excluding the youngest site (2003 burn), for a similar-aged stand, L_e^O was significantly lower

Table 2 – Timing of key spring phenological events by site and cumulative growing-degree-days (ΣD, °C days) calculated with Eq. (4) and the canopy F_{IPAR} phenology data

Stand age (years)	Green-up, Mean (±S.D.)	Maturity, Mean (±S.D.)
1	459.0 (±36.5)	734.8 (±20.0)
10	335.8 (±15.4)	495.8 (±11.4)
15	281.1 (±39.2)	669.6 (±33.1)
23	374.4 (±58.8)	678.0 (±44.4)
40	406.1 (±80.5)	747.9 (±47.0)
74	502.5 (±25.0)	816.6 (±27.2)
154	439.0 (±30.0)	667.4 (±29.0)
Average (Deciduous)	362.6 (±75.0)	644.6 (±103.3)
Average (Conifer)	470.7 (±45.0)	742 (±105.5)
Average (All)	400.0 (±75.8)	687.2 (±100.1)

ΣD are the summation of every degree day above the base temperature (0 °C) beginning 1st January. The average of the deciduous sites represents the average for the 23-year-old and younger burns sites, while the 1930 and 1850 burns are shown as the conifer average. Values in parentheses represent one standard deviation.

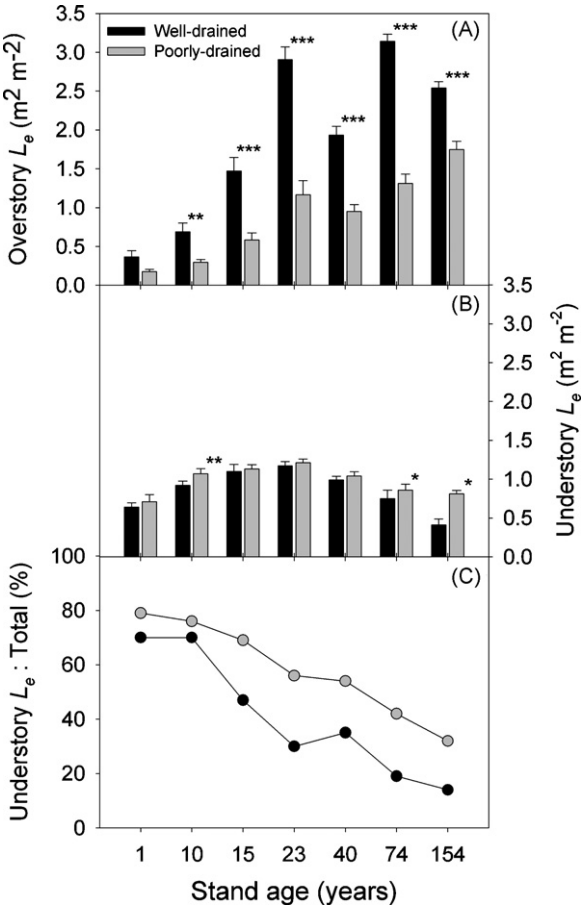

Fig. 5 – The variation of L_e across the chronosequence for the overstory (A) and understory (B) within the well- and poorly-drained stands. The bottom graph (C) shows the relative contribution of the understory L_e to the total for each wet and dry stand comprising the chronosequence. *P < 0.05, **0.01 < P < 0.05, ***0.005 < P < 0.01 for comparison between well- and poorly-drained stands.

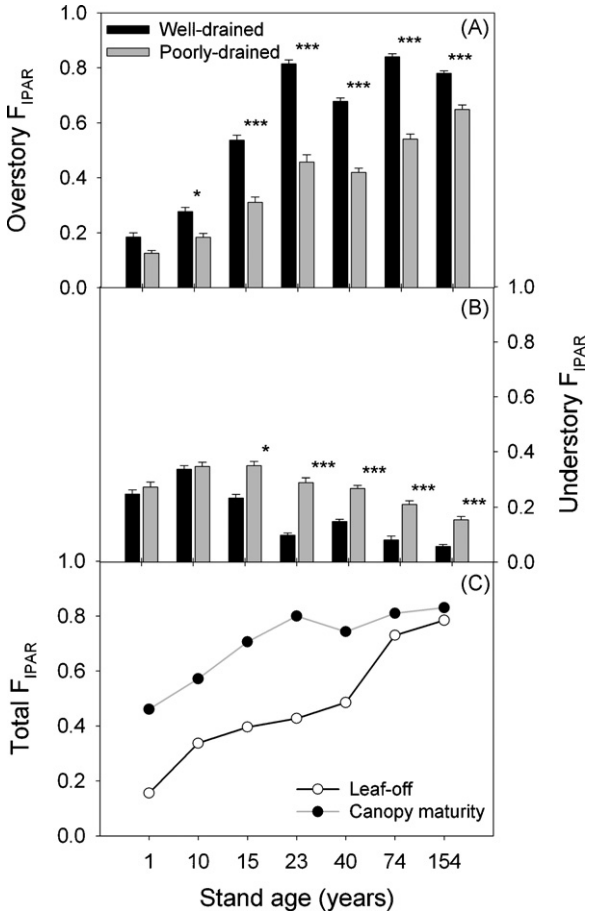

Fig. 6 – The variation of F_{IPAR} across the chronosequence for the overstory (A) and understory (B) within the well- and poorly-drained stands. The bottom graph (C) illustrates the seasonal change in total F_{IPAR} (F^T_{IPAR}) from leaf-off to maximum growing season values, by stand age. *P < 0.05, **0.01 < P < 0.05, ***0.005 < P < 0.01 for comparison between well- and poorly-drained stands.

($p < 0.001$) for the poorly-drained than well-drained stands, and increased consistently with stand development (i.e. stand age) to a maximum of 1.75 ± 0.11 for the 154-year-old wet stands (Fig. 5A).

Understory L_e (L^U_e) exhibited a bell-shaped curve across the wildfire chronosequence and averaged 14% more for the poorly-drained than well-drained stands (Fig. 5B). L^U_e comprised an increasingly smaller fraction of the total L_e (L^T_e) during stand development in the poorly-drained stands and well-drained stands (Fig. 5C). A negative linear correlation was observed between stand age and the $L^U_e : L^T_e$ for both the well- ($R^2 = 0.62$, $p < 0.001$) and poorly-drained ($R^2 = 0.86$, $p < 0.001$) chronosequences (Fig. 5C).

L^T_e was significantly larger ($p < 0.01$) in the well-drained than poorly-drained stands, excluding the youngest ($p = 0.30$) stands. Together, stand age and soil drainage explained greater than 70% of the variation in L^O_e (RMSE = 0.64) and 63% of the variation in L^T_e (RMSE = 0.67) across the chronosequence. Stand age explained 43% and (RMSE = 0.83), and 44% of variation (RMSE = 0.85) in L^T_e and L^O_e, respectively.

Overstory F_{IPAR} increased with stand age (Fig. 6A), and reached a maximum (mean $\pm$ S.E.) of 0.84 ± 0.02 in the 74 (well-drained stand) and 0.65 ± 0.02 in the 154 (poorly-drained stand). In general, F^T_{IPAR} was greater for well-drained than poorly-drained stands, excluding the 1-year-old burn site. Conversely, F^U_{IPAR} generally exhibited the opposite correlation with stand age with the highest values in the youngest stands and decreasing by 56% to a minimum F^U_{IPAR} of 0.11 ± 0.1 in the 154-year-old stands (Fig. 6B).

3.4. *Spatial variation of L_e*

The coefficients of variation (CV) of LAI were significantly correlated to stand age ($R = 0.61$, $p < 0.001$) and generally decreased with increasing stand development. The average CV's for the 1- and 10-year-old stands averaged 93% and 48% for L^O_e and L^T_e, respectively, compared to 27% for L^O_e in the 154-year-old stands, and 21% for L^T_e in the 74-year-old stands (Fig. 7). Coefficients of variation were significantly lower ($p < 0.0001$) in the well-drained than poorly-drained

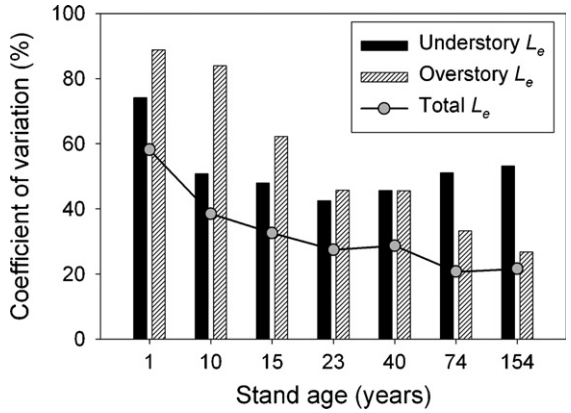

Fig. 7 – Coefficients of variation (CV) of L_e for the overstory, understory and total L_e by stand age.

stands (not shown). Within the youngest stands, overstory heterogeneity comprised a greater fraction of variation in L_e^T, whereas in the oldest stands, L_e^U was more variable (Fig. 7).

3.5. *Seasonal dynamics of L_e and F_{IPAR}*

Sites displayed significant seasonality in the stand-level L_e (Fig. 8). Both L_e^O and L_e^U increased significantly over the growing season ($p < 0.001$; Tukey's HSD test) for the 40-year-old and younger, deciduous and mixed stands. The 74-year-old stands had a much smaller, but nonetheless significant increase in L_e^O ($p = 0.006$) and L_e^U ($p < 0.001$). L_e^O did not differ significantly during the growing season for 154-year-old stand. For comparison, L_e^O averaged 4% greater for mid-summer (July) than the early spring (May) for the two oldest stands, whereas L_e^O averaged 70% great for mid-summer than early spring measurements for the 15- and 23-year-old stands (Fig. 8).

Understory L_e increased by 0.65 $m^2\,m^{-2}$ (79%) for the youngest stands, whereas peak L_e^U exceeded leafless values by 53% for the 10- and 15-year-old stands, 42% for the 40-year-old stands, and 58% for the understory vegetation in the 74- and 154-year-old stands. L_e^U varied over the growing season by 41% and 81% greater than L_e^O for the youngest stands (1994 and 2003 burn sites) and oldest stands (1930 and 1850) and only by 13% for the other three sites (1989–1964). Thus, the majority of the temporal variation in the stand-level L_e^T was attributed to the understory vegetation for the youngest and oldest stands.

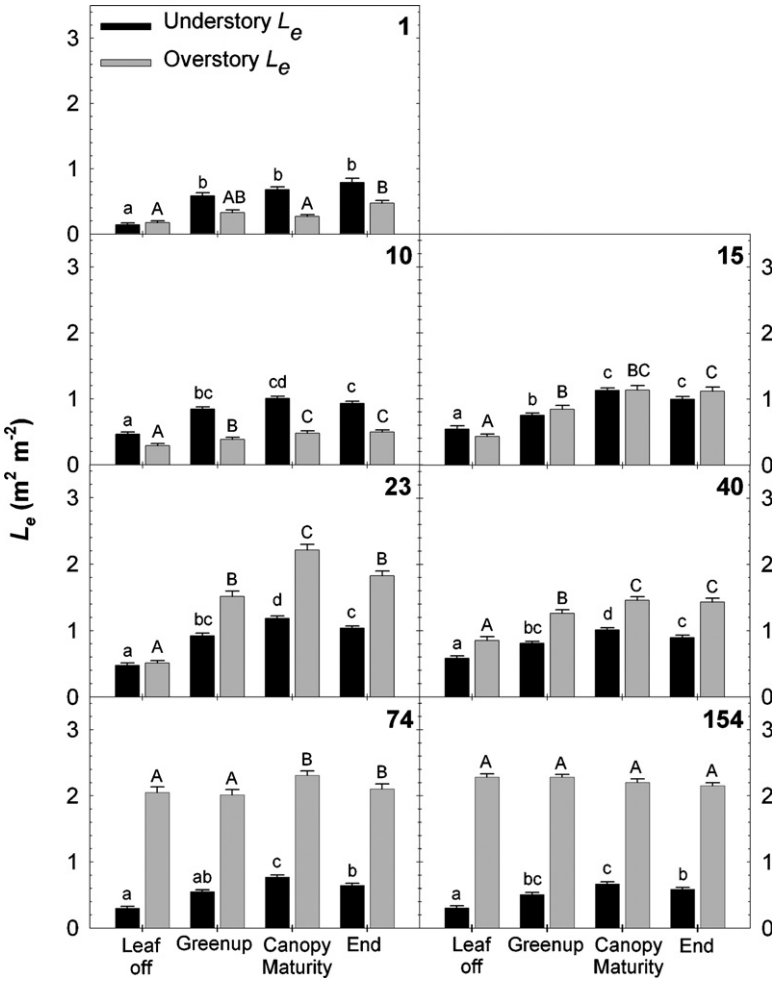

Fig. 8 – Seasonal patterns in the overstory and understory L_e for the chronosequence sites. Error bars represent the standard error of the site mean (combined well- and poorly-drained stands). Bars with similar lettering at not significantly different at the $\alpha = 0.05$ level.

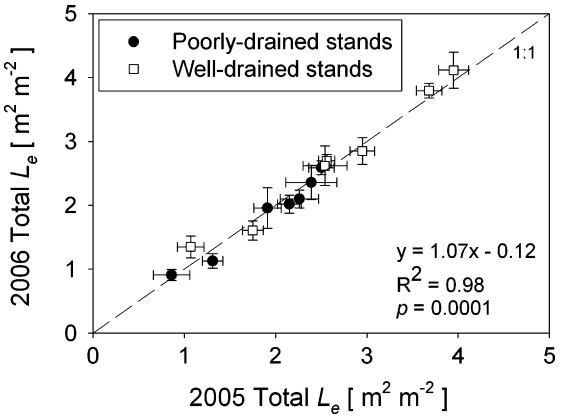

Fig. 9 – Inter-annual variation of L_e^T between the 2005 and 2006 growing seasons for the well- and poorly-drained stands. Error bars represent one standard error of the mean. Regression statistics are presented for the overall comparison between 2005 and 2006.

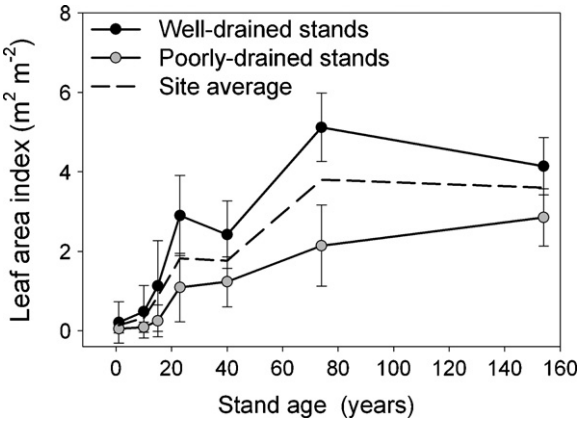

Fig. 10 – Stand level overstory leaf area index (LAI) for both the well- and poorly-drained stands investigated in this study. Error bars represent ± one standard deviation of the mean, and the site average is the arithmetic mean of the well- and poorly-drained stands.

Total F_{IPAR} increased significantly ($p < 0.001$) from leaf-off to maturity for the 40-year-old and younger stands or by an average of 0.33 (0.26–0.41) or 48% (Fig. 6). F_{IPAR}^T exhibited a much smaller increase (~9%) for the 154-year-old black spruce stands.

3.6. *Between-year variation*

The variation of L_e (and similarly F_{IPAR}) between 2005 and 2006 for all burn sites was minimal, averaging less than 14%, and the peak growing season L_e did not vary significantly between dry ($p = 0.85$) or wet stands ($p = 0.91$) (Fig. 9). We excluded the 2004 growing season due to the limited number of measurements for direct comparisons to the field measurements collected in 2005 and 2006. Overall, the 1-year-old site had the largest increase (~20%) in L_e^T, attributable to the increase in L_e^U during the 2006 growing season, where the greatest LAI accumulation occurred.

3.7. *Leaf area dynamics*

The contribution of α to L_e^O increased with stand age and ranged from 23% to 58% for the 23-year-old and younger stands. LAI steadily increased in the poorly-drained chronosequence, while for the well-drained chronosequence, LAI reached a maximum in the 74-year-old stand and declined (Fig. 10). LAI was significantly greater ($p < 0.001$) in the well-drained than similar aged poorly-drained stands and generally increased with stand age (Fig. 10). Along the well-drained chronosequence, LAI fell between (mean ± S.D.) 0.21 ± 0.52 and 4.14 ± 0.72, with a maximum LAI across the chronosequences of 5.12 ± 0.86 in the 74-year-old stand, followed by a significant decline ($p < 0.001$) to 4.14 154-year-old well-drained stand. The landscape scale estimates of LAI (i.e. the site average) exhibited an intermediate pattern to the well- and poorly-drained stands, and reached a peak of 3.8 in the 74-year-old stand.

4. Discussion

4.1. *Optical estimates of L_e and potential limitations*

Foliage clumping in boreal needle-leaf forests and to a lesser degree, deciduous broad-leaf forests is a key factor affecting the accuracy of optical LAI estimation (Gower et al., 1999; Jonckheere et al., 2004). An additional uncertainty may be the estimation of α, or the contribution of woody non-photosynthetic material in the canopy. Optical determination of this parameter is still in early stages of development (Kucharik et al., 1998; Chen et al., 2006b; Sonnentag et al., 2007). Furthermore, γ_E, and to a minor extent Ω of deciduous species (e.g. aspen) change seasonally (Chen, 1996; Chen et al., 1997a). Due to logistical constraints, and the difficulty in obtaining rapid spatial and temporal estimates of γ_E and Ω_E, we present maximum growing season LAI only. Additionally, it is LAI rather than L_e that is necessary for remote sensing and modeling applications. Our values are in reasonable agreement with those reported previously using a variety of LAI determination methods (Chen et al., 1997a,b, 2006b; Gower et al., 1997; Bond-Lamberty et al., 2002).

The LI-191SA radiation sensors provided important information on the timing and changes in canopy foliage. The sensors captured the differences in F_{IPAR} phenology of deciduous versus conifer canopies; however some difficulties were encountered. As previously reported (Gendron et al., 2001) variable cloudiness and inclement weather adversely affected the quantum sensor data. Some of our LI-191SA radiation sensors experienced periodic failure because they were not water-proof, resulting in loss of data and expensive instrument repair.

The number of sensors is important to the overall quality of data and patterns observed during the growing season. The number of micrometeorological stations equipped LI-191SA quantum sensors limited our spatial sampling; therefore, the exact values should be interpreted cautiously. Furthermore,

sensors were positioned 30 cm above the ground surface and therefore excluded the bryophyte and lichen ground layers. Bryophytes can dominate the carbon and nutrient cycling of poorly-drained areas in boreal forests (Turetsky, 2003) and Bond-Lamberty and Gower (2007) found that the ground cover vegetation (e.g. mosses, lichens) contributes a large fraction of the total LAI within these boreal stands. This exclusion is an important consideration to satellite validation studies where relatively open boreal forest canopies have a high background (understory, ground layer) reflectance that will contribute to the overall signal observed (Brown et al., 2000).

4.2. *Stand-level patterns of LAI and F_{IPAR}*

The LAI values and stand development patterns reported in this study support results from previous studies. Gower et al. (1997), using site-specific allometric equation, estimated the LAI of the154-year-old stands to be 4.2 compared to 4.1 (this study). Bond-Lamberty et al. (2002), using species-specific composite allometric equations, derived overstory LAI estimates for well- and poorly-drained stands in the chronosequence and they differed by 10–91% from this study. The differences in LAI between the two studies may be attributed to the greater spatial sampling used in this study. A more probable explanation is the younger stands increased in LAI during the past 5–7 years. The L_e^O for the 154-year-old stand (Northern Old Black Spruce Stand (NOBS) of 2.21 ± 0.73 was similar to the mean of ~2.31 reported for the 300 m area extending from the tower (Chen, 1996; Chen and Cihlar, 1996).

The age-dependent pattern in LAI and F_{PAR} (see Figs. 6 and 10) corroborates previously reported stand development patterns of LAI (Gower et al., 1996; Ryan et al., 1997). The decrease in L_e^T from the peak in the 23-year-old, primarily deciduous stands, to the oldest black spruce dominated stands (Fig. 5) was likely a consequence of the higher foliage clumping in the latter, not lower canopy LAI in the black spruce stands (Chen et al., 1997b). Bond-Lamberty et al. (2002) found that the overstory LAI peaked in the 1930 burn well-drained stands while total LAI was highest in the oldest black spruce stands (1930 and 1850 burns). Accounting for foliage clumping and the contribution of woody non-photosynthetic material in the optical measurements provided the expected successional pattern of LAI (Fig. 10).

Soil edaphic conditions influence overstory and understory species composition and LAI of boreal forests (Bisbee et al., 2001; Bond-Lamberty et al., 2002; Wang et al., 2003). Overstory and total L_e and F_{IPAR} were lower in poorly-drained than well-drained stands (Figs. 5 and 6). For example, the average L_e^O was 58% less in the 74-year-old poorly-drained stands than well-drained stands. This is comparable to the stand-age effect on canopy architecture. The opposite trend was observed for the understory, with generally higher L_e^U and F_{IPAR}^U values in the poorly-drained stands, coincident with a more open overstory canopy, in-turn resulting in a more favorable light environment for the understory vegetation.

4.3. *The role of understory*

Understory L_e and F_{IPAR} greatly varied across the chronosequence (Figs. 5–7) in response to overstory canopy structure, which changed during stand development (Table 1, Fig. 5A). Others have reported a rapid recovery of leaf area of stands originating from stand-killing wildfires (Bond-Lamberty et al., 2002; Goetz et al., 2006; Goulden et al., 2006). The variation of the understory vegetation found in the differing environmental conditions and stages of stand development illustrates the need to better understand and simulate understory vegetation dynamics of boreal forests. Understory vegetation influences radiation regime (Blanken et al., 1997; Barr et al., 2004) and carbon and nutrient cycles of boreal forests (Gower et al., 1997; Vogel and Gower, 1998; O'Connell et al., 2003).

Given the change in species composition observed with increasing stand age (Table 1), the successional change from deciduous or mixed stands to predominantly black spruce limits understory development (Figs. 5 and 6). The understory vegetation, such as herbaceous and woody shrubs, contributed largely to the L_e^T in the youngest stands, and generally comprised a higher proportion in the poorly-drained areas (Fig. 5). This is a function of the relatively sparse, open overstory canopy (mean $L_e \sim 1.14$) which is also highly variable (S.D. ~ 1.1); the F_{IPAR}^O values (Wet ~ 0.31, Dry ~ 0.54) were indicative of the high growing season transmittance of PAR in the youngest sites, even when fully leafed (Fig. 6). Also, the high degree of foliage clumping in mature boreal black spruce forests increases the fraction of radiation reaching the forest floor relative to a similar LAI with a uniform distribution (Chen et al., 1997b; Gower et al., 1999). This high degree of radiation transmission to the understory vegetation in early successional boreal forests has implications for understory development and succession (Ross et al., 1986).

L_e^U changed significantly during the year (Fig. 8) and was attributed to new foliage growth of the deciduous shrub and seasonal herbaceous species. The degree of canopy openness across all stands increases the reflectance signal from the understory and ground cover vegetation that changes significantly over the growing season (Miller et al., 1997). This relatively large seasonality in understory vegetation in black spruce stands likely explains the observed vegetative cycles over boreal spruce stands recorded with remotely sensed LAI data (e.g. Yang et al., 2006).

4.4. *Spatial variation of boreal forest canopy characteristics*

Variations of measured canopy characteristics were influenced by the stage of stand development, edaphic conditions and topography (not shown). Coefficients of variation were greater for the poorly-drained (mean = 82%) than the well-drained stands (mean = 62%) studied (Fig. 7). The more heterogeneous nature of the overstory canopy of the poorly-drained stands are likely caused by limited canopy closure, lower basal area, and reduced tree height and crown size (Bisbee et al., 2001; Bond-Lamberty et al., 2002). Burn severity contributes to the heterogeneous nature and successional dynamics of vegetation in the boreal forest, where within the young regrowth stands, the colonization of deciduous species (e.g. aspen and willow) occurs more frequently on the high-severity burned areas (Greene et al., 2004; Johnstone and Chapin, 2006a). Both L_e and F_{IPAR} were most variable in the youngest stands (1989–2003 burns) with coefficients of varia-

tion greater than 50% (Fig. 7). The general decrease in variation in the 23-year and older stands is attributed to the greater canopy closure and the conversion to black spruce dominance in the overstory (Table 1).

4.5. Inter-annual and seasonal variation in LAI and F_{IPAR}

Seasonal development of LAI is tightly coupled to net ecosystem production (NEP) of boreal forests (Black et al., 2000; Barr et al., 2004). As hypothesized, the mixed/deciduous stands exhibited the largest growing season changes in L_e while the oldest stands (1930 and 1850 burn sites) exhibited only minor (6–14%) detectable seasonal variation in the older stands. Leblanc and Chen (2001) reported an average seasonal change in L_e of 76% for deciduous stands in Ontario, Canada. Barr et al. (2004) reported large seasonal changes in LAI, increasing from leafless to an average annual maximum of 4.43 ± 0.56 for a boreal aspen/hazelnut stand. Conversely, Chen (1996) reported a variation in black spruce L_e of 5% seasonally for the Northern Old Black Spruce (NOBS) forest and 14% at the Southern Old Black Spruce Forest (SOBS). On average black spruce trees at the BOREAS northern and southern black spruce stands have an average leaf turnover (total foliage mass/new foliage mass) of approximately 12 years (Gower et al., 1997) and the small degree of new foliage growth generally occurs near the top of the crown, which is not easily measured with ground-based optical measurements. Moreover, the extremely high foliage clumping characteristic of boreal black spruce trees limits the detection of needle growth within the crown (Kucharik et al., 1999). Chen (1996) reported that the measurement error of optical instruments used to measure L_e ranged from 15 to 40%. It is important to note that these measurement errors exceed the small seasonal changes in mature black spruce stands studied and illustrates the difficult challenge of quantifying seasonal dynamics of foliage or early green-up for boreal landscapes dominated by spruce, or any other conifer with long-lived needles.

For a given stand, inter-annual variation in L_e was small and ranged from a minimum of 0.5 to a peak 20% for the 74- and 1-year-old stands, respectively. The inter-annual variation in the mean L_e (Fig. 9) and F_{IPAR} was less than the variation within individual burn sites, suggesting that spatial variation far exceeds the small inter-annual variation we observed during the 3-year study. From these field data and personal observations, LAI appeared to increase in the youngest stands from the 2004 to 2006 growing seasons, albeit the disparity in sample size limits direct conclusions to be drawn from this observed difference. We would expect a comparably lower LAI and reduced seasonality during the 2004 growing season, compared to 2006, in response to the cool, dry conditions that were observed across the boreal region of Canada (Bergeron et al., 2007).

4.6. Inter-annual and seasonal F_{IPAR} phenology

Species composition and structure affect the extent of seasonal change of canopy vegetation phenology observed, evident in the distinct differences between the deciduous and coniferous canopies (Fig. 3). Ahl et al. (2006) used a similar approach to derive phenological trajectories of temperate forest vegetation, *in situ*. Surprisingly few ground-based studies have examined the seasonality of vegetation in boreal ecosystems (Barr et al., 2004; Steinberg et al., 2006) where large disturbances (fire, insects, harvests) affect the variation in stand ages and species composition (Kurz and Apps, 1995), which influences vegetation dynamics across the landscape (Peckham et al., 2008).

Green-up was not clearly correlated to species composition or stand age, although the aspen dominated and mixed stands (1989–1964 burn sites) began greening up first (see Figs. 3 and 4), and had a lower calculated ΣD requirement (Table 2). The uncertainty in deriving canopy phenology transition dates was generally higher in the older than younger stands (see Fig. 4 error bars) as the degree of change in F_{IPAR} and variability in the data generally decreased and increased, respectively, with stand age and successional species. The delayed green-up of 24 and 27 days for the 15- and 40-year-old deciduous and mixed sites, respectively, in 2004 than 2005 and 2006, is likely correlated to the cooler, drier conditions and late spring warming (Bergeron et al., 2007). Mean air temperatures, measured at the NOBS (1850 burn site) micrometeorological and eddy covariance tower, were −1.8 and 3.6 °C for April and May 2004, 3.7 and 9.46 °C for April and May 2005, and 5.6 and 7.96 °C for April and May 2006. Bronson et al. (under review) reported that control black spruce trees broke bud about 21 days earlier in 2005 than 2004 (Fig. 4, open triangles).

We observed a positive relationship for the three years between the modeled dates of mean canopy green-up and maturity and the ΣD (Table 2), owing to the importance of thermal control of vegetation phenology in boreal forest stands (Linkosalo et al., 2006). The inter-annual differences in canopy F_{IPAR} phenology were generally correlated to spring-time differences in ΣD—a finding consistent with LAI phenology at the BOREAS southern study area mature aspen site (Barr et al., 2004). However, our ΣD threshold values were higher than those reported by Barr et al. Green-up was generally insensitive to the number of chilling days using the scheme of Botta et al. (2000), suggesting that chilling requirement is negligible for predicting green-up, given that boreal forests generally meet the chilling-day requirement (Barr et al., 2004; Linkosalo et al., 2006; Bronson et al., under review). The larger values of ΣD for the youngest 2003 burn site may be related to the dominant successional species present (i.e. comprised of understory vegetation) at this site, and the difficulty of quantifying the phenology of the low stature vegetation. Barr et al. (2004) found that green-up occurred about 92 °C days earlier for aspen than the hazelnut understory. Peckham et al. (2008) reported that green-up occurred later for 10-year-old or younger stands than 20-year-old post-fire stands across boreal Canada. We speculate that earlier green-up in the 20-year-old burns may be explained by the presence of aspen which is one of the first species to leaf-out (Lechowicz, 1984; Beaubien and Freeland, 2000). Finally, our estimate of 471 °C days for black spruce green-up is about 8% less than that observed by Bronson et al. (under review) for bud break in unheated, control plots (CO treatment).

4.7. Implications for remote sensing and modeling

The results presented in this study have important implications for mapping LAI and F_{PAR} for the boreal forests because these two key parameters are routinely used in ecosystem

biogeochemical process models to estimate energy, carbon and water budgets for terrestrial ecosystems. The accurate modeling of the reflectance signal from each vegetation strata is critical to accurately retrieving the surface information for validation, ecological modeling, and monitoring the dynamics of the landscape. All vegetation components (overstory, understory, bryophytes) and soil background contribute to the overall signal recorded by earth observing satellites (e.g. Eklundh et al., 2001; Shabanov et al., 2003; Eriksson et al., 2006). We conclude it is critical to measure the understory vegetation and characterize its seasonal canopy dynamics to understand spectral reflectance data from wildfire-dominated boreal landscapes. Accurate modeling of radiation in boreal canopies will require information on the canopy gap fractions estimated for the overstory and understory canopy strata transmission (Shabanov et al., 2003; Huang et al., 2007; Stenberg, 2007).

Understory vegetation, including bryophytes, is important to satellite studies of vegetation phenology in boreal forests. Seasonal changes in understory have been shown to influence the reflectance of boreal forests (Chen and Cihlar, 1996; Miller et al., 1997) and differing stand edaphic conditions leads to differences in leaf traits between the wet and dry stands. In our study region poorly-drained stands tend to contain evergreen understory species such as Labrador tea, whereas the well-drained stands generally contained deciduous shrub and seasonal herbaceous species. Few satellite-based studies of vegetation phenology in temperate and boreal forests have attempted to account for understory vegetation contribution (but see Ahl et al., 2006; Steinberg et al., 2006), while ground cover (mosses, lichens) vegetation have yet to be included. This represents a challenge for remote observation as the scale is often too coarse (e.g. 250, 500, 1000 m) to successfully separate the varying spatial and temporal patterns of the important canopy strata, although new techniques seem promising (e.g. Sonnentag et al., 2007).

A further complication to the decoupling of the direct and indirect effects of climate change on boreal vegetation phenology is the difficulty in measuring the fractional increase in needle-leaf area for black spruce and other boreal evergreen coniferous species that have extremely long-lived needles. The phenological dynamics of black spruce is difficult, if not impossible, to quantify indirectly with optical instruments because of the large noise-to-signal ratio (e.g. Chen, 1996; Steinberg et al., 2006). Our ground measurements provide some indication of the seasonality of black spruce stands (Figs. 3 and 8); however the uncertainty in the optical measurements currently limits the utility of these methods. This measurement challenge is relevant to studies attempting to correlate climate change to boreal forest phenology (e.g. Myneni et al., 1997; Slayback et al., 2003). We suggest that future studies take this into consideration when validating satellite data and interpreting greenness trends in boreal forests.

Currently, most ecosystem models that include LAI and F_{PAR} as state variables for estimating carbon budgets of boreal forests do not explicitly account for the LAI of understory and bryophyte vegetation (e.g. BIOME-BGC). However, bryophytes may contribute up to 50% of stand NPP in boreal forests and even a greater percentage of total NPP in boreal woodlands and peatlands (Gower et al., 2001). We recommended that modeling studies incorporate information on the understory vegetation, including bryophytes to improve the estimates of carbon and energy cycling in these stands. Many of these models use light use efficiency (LUE) coefficients to estimate NPP. However, instantaneous LUE coefficients can differ by more than 10-fold among overstory trees, understory and bryophytes (Whitehead and Gower, 2001). O'Connell et al. (2003) reported the average growing season LUE for bryophytes, understory, and overstory differed by 39 and 43% for poorly-drained and well-drained black spruce ecosystems at the BOREAS southern study area. These large differences in LUE among vegetation strata and the large differences in these strata's contribution to LAI seasonally during stand development illustrate the potential errors when estimating NPP for boreal landscapes. We conclude that reliable estimates of boreal forest and peatland carbon budgets are dependent upon proper understanding of the phenological patterning of both the overstory and understory vegetation. The influence of fire on landscape dynamics and phenology is still unclear and increased disturbance may negatively affect carbon storage (e.g. Thornley and Cannell, 2004; Bond-Lamberty et al., 2007).

5. Summary and conclusions

Stand age, soil edaphic conditions, and seasonal patterns influence LAI and F_{PAR} in boreal forests. Understory LAI development is inversely related to overstory LAI and can comprise a significant fraction of total LAI in these forests. Furthermore, understory vegetation can comprise the dominant fraction of seasonality in young and mature boreal forests. Detecting small changes in seasonal canopy dynamics, using optical ground-based or satellite-based measurements, is made extremely difficult for spruce-dominated boreal forests because of the heterogeneous canopy, non-random distribution of foliage and small turnover of needles.

Acknowledgements

This research was supported by a grant from US National Aeronautics and Space Administration (NNG04GL26G) to S.T. Gower and D.E. Ahl. Collection of the 2004–2005 NOBS data was funded by the US National Aeronautics and Space Administration (NAG5-11154 and NNG05GA76G). Collection of the 2005–2006 NOBS data was funded through the FLUXNET Canada Research Network by the Canadian Natural Sciences and Engineering Research Council (NSERC), the Canadian Foundation for Climate and Atmospheric Sciences and the BIOCAP Canada Foundation. We are grateful to the numerous undergraduate field assistants, to numerous to mention here, who's dedicated help made this research possible. We are indebted to Bruce Holmes of the Manitoba Department of Natural Resources for advice and necessary permits, and are additionally indebted to the Nisichawayasihk First Nation for permission to collect data on tribal land. Finally, we thank two anonymous reviewers for their helpful comments and suggestions which greatly improved earlier versions of this manuscript.

Appendix A. Seasonal periodic measurements of L_e and F_{IPAR}

Site	Year	Period	L_e Overstory		L_e Understory		F_{IPAR} Overstory		F_{IPAR} Understory	
			Mean	S.D. (error)	Mean	S.D. (error)	Mean	S.D. (error)	Mean	S.D. (error)
2003	2004	Leaf-off	0.21	0.15 (0.02)	–	–	0.13	0.09 (0.01)	–	–
		Green-up	0.15	0.15 (0.02)	0.37	0.32 (0.19)	0.12	0.08 (0.01)	0.17	0.16 (0.09)
		Max	0.26	0.16 (0.02)	0.29	0.40 (0.07)	0.18	0.08 (0.01)	0.14	0.16 (0.03)
		End	0.35	0.33 (0.04)	0.60	0.54 (0.12)	0.23	0.14 (0.02)	0.26	0.20 (0.04)
2003	2005	Max	0.24	0.38 (0.04)	0.62	0.60 (0.06)	0.13	0.15 (0.01)	0.26	0.19 (0.02)
2003	2006	Leaf-off	0.17	0.19 (0.03)	0.14	0.19 (0.03)	0.11	0.11 (0.02)	0.09	0.13 (0.02)
		Green-up	0.33	0.41 (0.04)	0.59	0.45 (0.05)	0.17	0.17 (0.02)	0.25	0.16 (0.02)
		Max	0.30	0.37 (0.04)	0.75	0.53 (0.05)	0.16	0.17 (0.02)	0.30	0.17 (0.02)
		End	0.47	0.41 (0.04)	0.79	0.61 (0.06)	0.26	0.19 (0.02)	0.30	0.20 (0.02)
1994	2004	Leaf-off	0.27	0.31 (0.05)	0.160	0.46 (0.07)	0.16	0.15 (0.02)	0.26	0.16 (0.03)
		Green-up	0.50	0.25 (0.04)	0.24	0.25 (0.04)	0.14	0.13 (0.02)	0.13	0.13 (0.02)
		Max	0.61	0.40 (0.06)	0.47	0.32 (0.05)	0.32	0.18 (0.02)	0.18	0.12 (0.02)
		End	0.63	0.54 (0.07)	0.94	0.56 (0.09)	0.32	0.23 (0.03)	0.34	0.18 (0.03)
1994	2005	Leaf-off	0.28	0.32 (0.05)	0.44	0.27 (0.06)	0.16	0.15 (0.02)	0.22	0.11 (0.02)
		Green-up	0.36	0.45 (0.04)	0.87	0.57 (0.05)	0.19	0.21 (0.02)	0.34	0.20 (0.02)
		Max	0.52	0.47 (0.04)	1.02	0.54 (0.05)	0.27	0.19 (0.02)	0.36	0.17 (0.01)
		End	0.46	0.46 (0.04)	0.92	0.47 (0.04)	0.25	0.20 (0.02)	0.34	0.15 (0.01)
1994	2006	Leaf-off	0.27	0.37 (0.05)	0.48	0.29 (0.04)	0.15	0.18 (0.02)	0.23	0.14 (0.02)
		Green-up	0.35	0.49 (0.04)	0.82	0.52 (0.04)	0.18	0.21 (0.02)	0.32	0.19 (0.02)
		Max	0.35	0.49 (0.04)	0.99	0.59 (0.05)	0.18	0.21 (0.02)	0.37	0.18 (0.01)
		End	0.50	0.54 (0.05)	0.94	0.53 (0.04)	0.24	0.22 (0.02)	0.34	0.18 (0.01)
1989	2004	Leaf-off	0.28	0.24 (0.03)	0.63	0.46 (0.07)	0.17	0.12 (0.02)	0.27	0.16 (0.02)
		Green-up	0.51	0.40 (0.05)	0.42	0.31 (0.04)	0.28	0.16 (0.02)	0.18	0.13 (0.02)
		Max	1.09	0.68 (0.09)	0.67	0.44 (0.07)	0.48	0.22 (0.03)	0.19	0.13 (0.02)
		End	1.04	0.76 (0.10)	0.76	0.54 (0.14)	0.46	0.24 (0.03)	0.28	0.18 (0.05)
1989	2005	Leaf-off	0.41	0.36 (0.05)	0.46	0.17 (0.04)	0.23	0.16 (0.02)	0.02	0.09 (0.02)
		Green-up	0.72	0.69 (0.07)	0.61	0.30 (0.04)	0.33	0.30 (0.04)	0.26	0.16 (0.02)
		Max	1.20	1.03 (0.08)	1.18	0.60 (0.05)	0.47	0.27 (0.02)	0.30	0.19 (0.02)
		End	0.99	0.83 (0.08)	0.94	0.51 (0.05)	0.43	0.25 (0.02)	0.27	0.17 (0.02)
1989	2006	Leaf-off	0.46	0.39 (0.06)	0.58	0.46 (0.06)	0.25	0.17 (0.02)	0.24	0.18 (0.03)
		Green-up	0.92	0.94 (0.08)	0.83	0.56 (0.05)	0.38	0.29 (0.02)	0.27	0.20 (0.02)
		Max	1.10	1.23 (0.10)	1.09	0.57 (0.05)	0.41	0.31 (0.03)	0.29	0.18 (0.02)
		End	1.19	1.13 (0.09)	1.05	0.71 (0.06)	0.45	0.29 (0.02)	0.28	0.21 (0.02)
1981	2004	Leaf-off	0.69	0.44 (0.08)	0.59	0.34 (0.07)	0.35	0.17 (0.03)	0.20	0.10 (0.02)
		Green-up	0.55	0.33 (0.04)	0.44	0.26 (0.03)	0.31	0.15 (0.02)	0.18	0.09 (0.01)
		Max	0.98	0.73 (0.11)	0.91	0.51 (0.12)	0.44	0.23 (0.04)	0.30	0.16 (0.04)
1981	2005	Leaf-off	0.54	0.33 (0.05)	0.39	0.17 (0.04)	0.29	0.15 (0.02)	0.02	0.09 (0.02)
		Green-up	0.98	0.71 (0.08)	0.93	0.47 (0.06)	0.43	0.26 (0.03)	0.28	0.18 (0.02)
		Max	2.13	1.22 (0.12)	1.12	0.55 (0.05)	0.68	0.26 (0.02)	0.17	0.16 (0.02)
		End	1.74	1.17 (0.10)	0.97	0.45 (0.04)	0.59	0.29 (0.02)	0.19	0.15 (0.01)
1981	2006	Leaf-off	0.47	0.42 (0.05)	0.50	0.33 (0.04)	0.24	0.19 (0.02)	0.21	0.15 (0.02)
		Green-up	1.81	1.29 (0.11)	0.91	0.64 (0.06)	0.60	0.32 (0.03)	0.17	0.17 (0.01)
		Max	2.20	1.5 (0.13)	1.24	0.57 (0.05)	0.65	0.30 (0.03)	0.19	0.17 (0.01)
		End	1.91	1.25 (0.10)	1.10	0.53 (0.04)	0.62	0.30 (0.03)	0.19	0.17 (0.01)
1964	2004	Leaf-off	0.64	0.51 (0.07)	0.57	0.30 (0.04)	0.32	0.20 (0.03)	0.20	0.11 (0.02)
		Green-up	0.96	0.65 (0.08)	0.45	0.32 (0.05)	0.43	0.24 (0.03)	0.16	0.14 (0.02)
		Max	1.10	0.78 (0.10)	0.57	0.28 (0.04)	0.46	0.23 (0.03)	0.17	0.10 (0.01)
		End	1.38	0.98 (0.08)	0.90	0.55 (0.08)	0.53	0.27 (0.02)	0.29	0.22 (0.03)
1964	2005	Leaf-off	0.86	0.74 (0.08)	0.52	0.37 (0.10)	0.37	0.24 (0.03)	0.22	0.18 (0.05)
		Green-up	1.37	0.94 (0.08)	0.79	0.45 (0.04)	0.52	0.27 (0.02)	0.21	0.18 (0.02)
		Max	1.51	0.88 (0.07)	1.03	0.56 (0.04)	0.58	0.22 (0.02)	0.21	0.15 (0.01)
1964	2006	Leaf-off	0.77	0.54 (0.08)	0.60	0.27 (0.04)	0.38	0.20 (0.03)	0.20	0.09 (0.01)
		Green-up	1.10	0.87 (0.08)	0.83	0.38 (0.03)	0.45	0.26 (0.02)	0.23	0.15 (0.01)
		Max	1.37	0.97 (0.08)	0.99	0.55 (0.05)	0.53	0.24 (0.02)	0.23	0.16 (0.01)
		End	1.34	0.99 (0.08)	0.91	0.63 (0.05)	0.51	0.25 (0.02)	0.23	0.20 (0.02)

Appendix A (*Continued*)

Site	Year	Period	L_e Overstory		L_e Understory		F_{IPAR} Overstory		F_{IPAR} Understory	
			Mean	S.D. (error)	Mean	S.D. (error)	Mean	S.D. (error)	Mean	S.D. (error)
1930	2004	Leaf-off	1.82	0.88 (0.12)	0.86	1.16 (0.58)	0.64	0.25 (0.04)	0.16	0.19 (0.09)
		Green-up	2.02	0.85 (0.12)	0.39	0.15 (0.04)	0.68	0.21 (0.03)	0.11	0.10 (0.02)
		Max	2.52	0.92 (0.13)	0.60	0.40 (0.11)	0.77	0.20 (0.03)	0.16	0.17 (0.05)
		End	2.96	0.94 (0.13)	–	–	0.83	0.11 (0.02)	–	–
1930	2005	Leaf-off	1.88	1.01 (0.12)	0.36	0.25 (0.11)	0.63	0.26 (0.03)	0.11	0.07 (0.03)
		Green-up	1.72	1.07 (0.11)	0.64	0.41 (0.06)	0.59	0.28 (0.03)	0.23	0.18 (0.03)
		Max	2.28	1.22 (0.10)	0.92	0.51 (0.06)	0.69	0.26 (0.02)	0.22	0.18 (0.02)
		End	2.04	1.06 (0.12)	0.68	0.31 (0.04)	0.66	0.22 (0.02)	0.15	0.11 (0.01)
1930	2006	Leaf-off	2.29	0.87 (0.12)	0.30	0.20 (0.03)	0.73	0.19 (0.03)	0.05	0.05 (0.01)
		Green-up	2.19	1.26 (0.10)	0.52	0.40 (0.03)	0.67	0.30 (0.02)	0.12	0.17 (0.01)
		Max	2.33	1.22 (0.10)	0.70	0.50 (0.04)	0.70	0.24 (0.02)	0.18	0.15 (0.01)
		End	2.13	1.18 (0.10)	0.64	0.47 (0.04)	0.67	0.26 (0.02)	0.13	0.16 (0.01)
1850	2004	Leaf-off	2.10	0.58 (0.10)	0.53	0.45 (0.08)	0.73	0.11 (0.02)	0.07	0.06 (0.01)
		Green-up	2.52	0.78 (0.10)	0.42	0.28 (0.07)	0.80	0.18 (0.02)	0.07	0.06 (0.02)
		Max	2.24	0.51 (0.07)	0.47	0.28 (0.07)	0.75	0.10 (0.01)	0.10	0.06 (0.02)
1850	2005	Leaf-off	2.36	0.50 (0.07)	0.42	0.30 (0.07)	0.77	0.10 (0.01)	0.07	0.06 (0.02)
		Green-up	2.33	0.54 (0.05)	0.88	0.34 (0.08)	0.76	0.11 (0.01)	0.16	0.12 (0.03)
		Max	2.20	0.75 (0.07)	0.82	0.38 (0.07)	0.73	0.18 (0.02)	0.16	0.08 (0.02)
		End	2.20	0.65 (0.07)	0.55	0.29 (0.07)	0.74	0.13 (0.01)	0.13	0.07 (0.02)
1850	2006	Leaf-off	2.22	0.58 (0.07)	0.32	0.25 (0.03)	0.74	0.11 (0.01)	0.05	0.04 (0.01)
		Green-up	2.21	0.70 (0.08)	0.43	0.28 (0.03)	0.74	0.13 (0.01)	0.07	0.06 (0.01)
		Max	2.21	0.81 (0.07)	0.64	0.40 (0.04)	0.73	0.14 (0.01)	0.10	0.10 (0.01)
		End	2.15	0.68 (0.06)	0.58	0.34 (0.03)	0.73	0.13 (0.01)	0.09	0.07 (0.01)

REFERENCES

Ahl, D.E., Gower, S.T., Burrows, S.N., Shabanov, N.V., Myneni, R.B., Knyazikhin, Y., 2006. Monitoring spring canopy phenology of a deciduous broadleaf forest using MODIS. Rem. Sens. Environ. 104 (1), 88–95.

Amiro, B.D., Todd, J.B., Wotton, B.M., Logan, K.A., Flannigan, M.D., Stocks, B.J., Mason, J.A., Martell, D.L., Hirsch, K.G., 2001. Direct carbon emissions from Canadian forest fires 1959–1999. Can. J. For. Res. 31 (3), 512–525.

Amiro, B.D., Orchansky, A.L., Barr, A.G., Black, T.A., Chambers, S.D., Chapin, F.S., Gouldenf, M.L., Litvakg, M., Liu, H.P., Mccaughey, J.H., Mcmillan, A., Randerson, J.T., 2006. The effect of post-fire stand age on the boreal forest energy balance. Agric. For. Meteorol. 140 (1–4), 41–50.

Angert, A., Biraud, S., Bonfils, C., Henning, C.C., Buermann, W., Pinzon, J., Tucker, C.J., Fung, I., 2005. Drier summers cancel out the CO_2 uptake enhancement induced by warmer springs. Proc. Natl. Acad. Sci. 102 (31), 10823–10827.

Badeck, F.W., Bondeau, A., Bottcher, K., Doktor, D., Lucht, W., Schaber, J., Sitch, S., 2004. Responses of spring phenology to climate change. New Phyt. 162 (2), 295–309.

Barr, A.G., Black, T.A., Hogg, E.H., Kljun, N., Morgenstern, K., Nesic, Z., 2004. Inter-annual variability in the leaf area index of a boreal aspen-hazelnut forest in relation to net ecosystem production. Agric. For. Meteorol. 126 (3/4), 237–255.

Beaubien, E.G., Freeland, H.J., 2000. Spring phenology trends in Alberta, Canada: links to ocean temperature. Int. J. Biometeorol. 44 (2), 53–59.

Bergeron, O., Margolis, H.A., Black, T.A., Coursolle, C., Dunn, A.L., Barr, A.G., Wofsy, S.C., 2007. Comparison of carbon dioxide fluxes over three boreal black spruce forests in Canada. Global Change Biol. 13 (1), 89–107.

Bisbee, K.E., Gower, S.T., Norman, J.M., Nordheim, E.V., 2001. Environmental controls on ground cover species composition and productivity in a boreal black spruce forest. Oecologia 129 (2), 261–270.

Black, T.A., Chen, W.J., Barr, A.G., Arain, M.A., Chen, Z., Nesic, Z., Hogg, E.H., Neumann, H.H., Yang, P.C., 2000. Increased carbon sequestration by a boreal deciduous forest in years with a warm spring. Geophys. Res. Lett. 27 (9), 1271–1274.

Blanken, P.D., Black, T.A., Yang, P.C., Neumann, H.H., Nesic, Z., Staebler, R., Den Hartog, G., Novak, M.D., Lee, X., 1997. Energy balance and canopy conductance of a boreal aspen forest: partitioning overstory and understory components. J. Geophys. Res. Atmos. 102 (D24), 28915–28927.

Bogaert, J., Zhou, L., Tucker, C.J., Myneni, R.B., Ceulemans, R., 2002. Evidence for a persistent and extensive greening trend in Eurasia inferred from satellite vegetation index data. J. Geophys. Res. Atmos. 107 (D11).

Bonan, G.B., 1991. Seasonal and annual fluxes in a boreal forest landscape. J. Geophys. Res. 96, 17329–17338.

Bonan, G.B., 1993. Importance of leaf area index and forest type when estimating photosynthesis in boreal forests. Rem. Sens. Environ. 43, 303–314.

Bond-Lamberty, B., Gower, S.T., 2007. Estimation of stand-level leaf area for boreal bryophytes. Oecologia 151 (4), 584–592.

Bond-Lamberty, B., Wang, C., Gower, S.T., Norman, J., 2002. Leaf area dynamics of a boreal black spruce fire chronosequence. Tree Physiol. 22 (14), 993–1001.

Bond-Lamberty, B., Wang, C.K., Gower, S.T., 2004. Net primary production and net ecosystem production of a boreal black spruce wildfire chronosequence. Global Change Biol. 10 (4), 473–487.

Bond-Lamberty, B., Peckham, S.D., Ahl, D.E., Gower, S.T., 2007. Fire as the dominant driver of central Canadian boreal forest carbon balance. Nature 450 (7166), 89–93.

Botta, A., Viovy, N., Ciais, P., Friedlingstein, P., Monfray, P., 2000. A global prognostic scheme of leaf onset using satellite data. Global Change Biol. 6 (7), 709–725.

Bronson, D.R., Gower, S.T., Tanner, M., Van Herk, I., under review. Effect of ecosystem warming on boreal black spruce bud burst and shoot growth. Global Change Biol.

Brown, L., Chen, J.M., Leblanc, S.G., Cihlar, J., 2000. A shortwave infrared modification to the simple ratio for LAI retrieval in boreal forests: an image and model analysis. Rem. Sens. Environ. 71 (1), 16–25.

Buermann, W., Lintner, B.R., Koven, C.D., Angert, A., Pinzon, J.E., Tucker, C.J., Fung, I.Y., 2007. The changing carbon cycle at Mauna Loa Observatory. Proc. Natl. Acad. Sci. 104 (11), 4249–4254.

Bunn, A.G., Goetz, S.J., Fiske, G.J., 2005. Observed and predicted responses of plant growth to climate across Canada. Geophys. Res. Lett. 32 (16.).

Burrows, S.N., Gower, S.T., Clayton, M.K., Mackay, D.S., Ahl, D.E., Norman, J.M., Diak, G., 2002. Application of geostatistics to characterize leaf area index (LAI) from flux tower to landscape scales using a cyclic sampling design. Ecosystems 5 (7), 667–679.

Campbell, G.S., Norman, J.M., 1998. An Introduction to Environmental Biophysics. Springer, New York, p. 286.

Chapman, W.L., Walsh, J.E., 1993. Recent variations of sea ice and air-temperature in high-latitudes. Bull. Am. Meteorol. Soc. 74 (1), 33–47.

Chen, J.M., 1996. Optically-based methods for measuring seasonal variation of leaf area index in boreal conifer stands. Agric. For. Meteorol. 80 (2–4), 135–163.

Chen, J.M., Black, T.A., 1992. Defining leaf-area index for non-flat leaves. Plant Cell Environ. 15 (4), 421–429.

Chen, J.M., Cihlar, J., 1995. Quantifying the effect of canopy architecture on optical measurements of leaf-area index using 2 gap size analysis-methods. IEEE Trans. Geo. Rem. Sen. 33 (3), 777–787.

Chen, J.M., Cihlar, J., 1996. Retrieving leaf area index of boreal conifer forests using Landsat TM images. Rem. Sens. Environ. 55 (2), 153–162.

Chen, J.M., Blanken, P.D., Blank, T.A., Guilbeault, M., Chen, S., 1997a. Radiation regime and canopy architecture in a boreal aspen forest. Agric. For. Meteorol. 86 (1/2), 107–125.

Chen, J.M., Rich, P.M., Gower, S.T., Norman, J.M., Plummer, S., 1997b. Leaf area index of boreal forests: theory, techniques, and measurements. J. Geophys. Res. Atmos. 102 (D24), 29429–29443.

Chen, J.M., Chen, B.Z., Higuchi, K., Liu, J., Chan, D., Worthy, D., Tans, P., Black, A., 2006a. Boreal ecosystems sequestered more carbon in warmer years. Geophys. Res. Lett. 33 (10).

Chen, J.M., Govind, A., Sonnentag, O., Zhang, Y.Q., Barr, A., Amiro, B., 2006b. Leaf area index measurements at Fluxnet-Canada forest sites. Agric. For. Meteorol. 140 (1–4), 257–268.

Chuine, I., Cour, P., 1999. Climatic determinants of budburst seasonality in four temperate-zone tree species. New Phyt. 143 (2), 339–349.

Ciais, P., Tans, P.P., Trolier, M., White, J.W.C., Francey, R.J., 1995. A large northern-hemisphere terrestrial CO_2 sink indicated by the C-13/C-12 ratio of atmospheric CO_2. Science 269 (5227), 1098–1102.

Conard, S.G., Sukhinin, A.I., Stocks, B.J., Cahoon, D.R., Davidenko, E.P., Ivanova, G.A., 2002. Determining effects of area burned and fire severity on carbon cycling and emissions in Siberia. Climatic Change 55 (1/2), 197–211.

D'Arrigo, R., Jacoby, G.C., Fung, I.Y., 1987. Boreal forests and atmosphere-biosphere exchange of carbon dioxide. Nature 329, 321–323.

Dixon, K.R., 1976. Analysis of seasonal leaf fall in north temperate deciduous forests. Oikos 27.

Dunn, A.L., Barford, C.C., Wofsy, S.C., Goulden, M.L., Daube, B.C., 2007. A long-term record of carbon exchange in a boreal black spruce forest: means, responses to interannual variability, and decadal trends. Global Change Biol. 13 (3), 577–590.

Eklundh, L., Harrie, L., Kuusk, A., 2001. Investigating relationships between Landsat ETM + sensor data and leaf area index in a boreal conifer forest. Rem. Sens. Environ. 78 (3), 239–251.

Eriksson, H.M., Eklundh, L., Kuusk, A., Nilson, T., 2006. Impact of understory vegetation on forest canopy reflectance and remotely sensed LAI estimates. Rem. Sens. Environ. 103 (4), 408–418.

Fisher, J.I., Richardson, A.D., Mustard, J.F., 2007. Phenology model from surface meteorology does not capture satellite-based green-up estimations. Global Change Biol. 13 (3), 707–721.

Flannigan, M.D., Logan, K.A., Amiro, B.D., Skinner, W.R., Stocks, B.J., 2005. Future area burned in Canada. Climatic Change 72 (1/2), 1–16.

Frolking, S., Milliman, T., Mcdonald, K., Kimball, J., Zhao, M.S., Fahnestock, M., 2006. Evaluation of the SeaWinds scatterometer for regional monitoring of vegetation phenology. J. Geophys. Res. Atmos. 111 (D17).

Gendron, F., Messier, C., Comeau, P.G., 2001. Temporal variations in the understorey photosynthetic photon flux density of a deciduous stand: the effects of canopy development, solar elevation, and sky conditions. Agric. For. Meteorol. 106, 23–40.

Gobron, N., Pinty, B., Aussedat, O., Chen, J.M., Cohen, W.B., Fensholt, R., Gond, V., Huemmrich, K.F., Lavergne, T., Melin, F., Privette, J.L., Sandholt, I., Taberner, M., Turner, D.P., Verstraete, M.M., Widlowski, J.L., 2006. Evaluation of fraction of absorbed photosynthetically active radiation products for different canopy radiation transfer regimes: methodology and results using joint research center products derived from SeaWiFS against ground-based estimations. J. Geophys. Res. Atmos. 111 (D13).

Goetz, S.J., Bunn, A.G., Fiske, G.J., Houghton, R.A., 2005. Satellite-observed photosynthetic trends across boreal North America associated with climate and fire disturbance. Proc. Natl. Acad. Sci. 102 (38), 13521–13525.

Goetz, S.J., Fiske, G.J., Bunn, A.G., 2006. Using satellite time-series data sets to analyze fire disturbance and forest recovery across Canada. Rem. Sens. Environ. 101 (3), 352–365.

Goodale, C.L., Apps, M.J., Birdsey, R.A., Field, C.B., Heath, L.S., Houghton, R.A., Jenkins, J.C., Kohlmaier, G.H., Kurz, W., Liu, S.R., Nabuurs, G.J., Nilsson, S., Shvidenko, A.Z., 2002. Forest carbon sinks in the Northern Hemisphere. Ecol. Appl. 12 (3), 891–899.

Goulden, M.L., Wofsy, S.C., Harden, J.W., Trumbore, S.E., Crill, P.M., Gower, S.T., Fries, T., Daube, B.C., Fan, S.M., Sutton, D.J., Bazzaz, A., Munger, J.W., 1998. Sensitivity of boreal forest carbon balance to soil thaw. Science 279 (5348), 214–217.

Goulden, M.L., Winston, G.C., McMillan, A.M.S., Litvak, M.E., Read, E.L., Rocha, A.V., Elliot, J.R., 2006. An eddy covariance mesonet to measure the effect of forest age on land-atmosphere exchange. Global Change Biol. 12 (11), 2146–2162.

Gower, S.T., McMurtrie, R.E., Murty, D., 1996. Aboveground net primary production decline with stand age: potential causes. Trends Ecol. Evol. 11 (9), 378–382.

Gower, S.T., Vogel, J.G., Norman, J.M., Kucharik, C.J., Steele, S.J., Stow, T.K., 1997. Carbon distribution and aboveground net primary production in aspen, jack pine, and black spruce stands in Saskatchewan and Manitoba, Canada. J. Geophys. Res. Atmos. 102 (D24), 29029–29041.

Gower, S.T., Kucharik, C.J., Norman, J.M., 1999. Direct and indirect estimation of leaf area index, F_{PAR}, and net primary

production of terrestrial ecosystems. Rem. Sens. Environ. 70 (1), 29–51.
Gower, S.T., Krankina, O., Olson, R.J., Apps, M., Linder, S., Wang, C., 2001. Net primary production and carbon allocation patterns of boreal forest ecosystems. Ecol. Appl. 11 (5), 1395–1411.
Greene, D.F., Noel, J., Bergeron, Y., Rousseau, M., Gauthier, S., 2004. Recruitment of *Picea mariana*, *Pinus banksiana*, and *Populus tremuloides* across a burn severity gradient following wildfire in the southern boreal forest of Quebec. Can. J. For. Res. 34 (9), 1845–1857.
Huang, D., Knyazikhin, Y., Dickinson, R.E., Rautiainen, M., Stenberg, P., Disney, M., Lewis, P., Cescatti, A., Tian, Y.H., Verhoef, W., Martonchik, J.V., Myneni, R.B., 2007. Canopy spectral invariants for remote sensing and model applications. Rem. Sens. Environ. 106 (1), 106–122.
Johnstone, J.F., 2006. Response of boreal plant communities to variations in previous fire-free interval. Int. J. Wildland Fire 15 (4), 497–508.
Johnstone, J., Chapin, F., 2006a. Effects of soil burn severity on post-fire tree recruitment in boreal forest. Ecosystems 9 (1), 14–31.
Johnstone, J.F., Chapin, F.S., 2006b. Fire interval effects on successional trajectory in boreal forests of northwest Canada. Ecosystems 9 (2), 268–277.
Jonckheere, I., Fleck, S., Nackaerts, K., Muys, B., Coppin, P., Weiss, M., Baret, F., 2004. Review of methods for in situ leaf area index determination. Part I. Theories, sensors and hemispherical photography. Agric. For. Meteorol. 121 (1/2), 19–35.
Kasischke, E.S., Christensen, N.L., Stocks, B.J., 1995. Fire, global warming, and the carbon balance of boreal forests. Ecol. Appl. 5 (2), 437–451.
Keeling, C.D., Chin, J.F.S., Whorf, T.P., 1996. Increased activity of northern vegetation inferred from atmospheric CO_2 measurements. Nature 382 (6587), 146–149.
Kramer, K., 1994. Selecting a model to predict the onset of growth of fagus-sylvatica. J. Appl. Ecol. 31 (1), 172–181.
Kramer, K., Leinonen, I., Loustau, D., 2000. The importance of phenology for the evaluation of impact of climate change on growth of boreal, temperate and Mediterranean forests ecosystems: an overview. Int. J. Biometeorol. 44 (2), 67–75.
Kucharik, C.J., Norman, J.M., Gower, S.T., 1998. Measurements of branch area and adjusting leaf area index indirect measurements. Agric. For. Meteorol. 91 (1/2), 69–88.
Kucharik, C.J., Norman, J.M., Gower, S.T., 1999. Characterization of radiation regimes in nonrandom forest canopies: theory, measurements, and a simplified modeling approach. Tree Physiol. 19 (11), 695–706.
Kurz, W.A., Apps, M.J., 1995. An analysis of future carbon budgets of Canadian boreal forests. Water Air Soil Pollut. 82 (1/2), 321–331.
Kurz, W.A., Apps, M.J., 1999. A 70-year retrospective analysis of carbon fluxes in the canadian forest sector. Ecol. Appl. 9 (2), 526–547.
Kurz, W.A., Dymond, C.C., Stinson, G., Rampley, G.J., Neilson, E.T., Carroll, A.L., Ebata, T., Safranyik, L., 2008. Mountain pine beetle and forest carbon feedback to climate change. Nature 452 (7190), 987–990.
Leblanc, S.G., Chen, J.M., 2001. A practical scheme for correcting multiple scattering effects on optical LAI measurements. Agric. For. Meteorol. 110 (2), 125–139.
Lechowicz, M.J., 1984. Why do temperate deciduous trees leaf-out at different times-adaptation and ecology of forest communities. Am. Nat. 124 (6), 821–842.
Leinonen, I., Kramer, K., 2002. Applications of phenological models to predict the future carbon sequestration potential of boreal forests. Climatic Change 55 (1/2), 99–113.
LI-COR, 1991. Plant Canopy Analyzer Operating Manual. LI-COR Inc., Lincoln, NE.
Linkosalo, T., Hakkinen, R., Hanninen, H., 2006. Models of the spring phenology of boreal and temperate trees: is there something missing? Tree Physiol. 26 (9), 1165–1172.
Liu, H.P., Randerson, J.T., Lindfors, J., Chapin, F.S., 2005. Changes in the surface energy budget after fire in boreal ecosystems of interior Alaska: an annual perspective. J. Geophys. Res. Atmos. 110 (D13), 12.
Lucht, W., Prentice, I.C., Myneni, R.B., Sitch, S., Friedlingstein, P., Cramer, W., Bousquet, P., Buermann, W., Smith, B., 2002. Climatic control of the high-latitude vegetation greening trend and Pinatubo effect. Science 296 (5573), 1687–1689.
Martin, J.L., Gower, S.T., 2006. Boreal mixedwood tree growth on contrasting soils and disturbance types. Can. J. For. Res. 36 (4), 986–995.
Miller, J.R., White, H.P., Chen, J.M., Peddle, D.R., Mcdermid, G., Fournier, R.A., Shepherd, P., Rubinstein, I., Freemantle, J., Soffer, R., Ledrew, E., 1997. Seasonal change in understory reflectance of boreal forests and influence on canopy vegetation indices. J. Geophys. Res. Atmos. 102 (D24), 29475–29482.
Morisette, J.T., Baret, F., Privette, J.L., Myneni, R.B., Nickeson, J.E., Garrigues, S., Shabanov, N.V., Weiss, M., Fernandes, R.A., Leblanc, S.G., Kalacska, M., Sanchez-Azofeifa, G.A., Chubey, M., Rivard, B., Stenberg, P., Rautiainen, M., Voipio, P., Manninen, T., Pilant, A.N., Lewis, T.E., Iiames, J.S., Colombo, R., Meroni, M., Busetto, L., Cohen, W.B., Turner, D.P., Warner, E.D., Petersen, G.W., Seufert, G., Cook, R., 2006. Validation of global moderate-resolution LAI products: a framework proposed within the CEOS land product validation subgroup. IEEE Trans. Geo. Rem. Sen. 44 (7), 1804–1817.
Myneni, R.B., Keeling, C.D., Tucker, C.J., Asrar, G., Nemani, R.R., 1997. Increased plant growth in the northern high latitudes from 1981 to 1991. Nature 386 (6626), 698–702.
Notaro, M., Vavrus, S., Liu, Z.Y., 2007. Global vegetation and climate change due to future increases in CO_2 as projected by a fully coupled model with dynamic vegetation. J. Climate 20 (1), 70–90.
O'Connell, K.E.B., Gower, S.T., Norman, J.M., 2003. Net ecosystem production of two contrasting boreal black spruce forest communities. Ecosystems 6 (3), 248–260.
Peckham, S.D., Ahl, D.E., Serbin, S.P., Gower, S.T., 2008. Fire induced changes in start of growing season and leaf maturity in Canadian forests measured by satellite remote sensing. Rem. Sens. Environ. 112 (9), 3594–3603.
Penuelas, J., Filella, I., 2001. Phenology—responses to a warming world. Science 294 (5543), 793–795.
Potter, C., 2004. Predicting climate change effects on vegetation, soil thermal dynamics, and carbon cycling in ecosystems of interior Alaska. Ecol. Model. 175 (1), 1–24.
Ross, M.S., Flanagan, L.B., La Roi, G.H., 1986. Seasonal and successional changes in light quality and quantity in the understory of boreal forest ecosystems. Can. J. Bot. 64, 2792–2799.
Running, S.W., Nemani, R.R., Heinsch, F.A., Zhao, M.S., Reeves, M., Hashimoto, H., 2004. A continuous satellite-derived measure of global terrestrial primary production. Bioscience 54 (6), 547–560.
Ryan, M.G., Binkley, D., Fownes, J.H., 1997. In: Begon, M., Fitter, A.H. (Eds.), Age-related Decline in Forest Productivity: Pattern and Process. Academic Press, San Diego.
Shabanov, N.V., Wang, Y., Buermann, W., Dong, J., Hoffman, S., Smith, G.R., Tian, Y., Knyazikhin, Y., Myneni, R.B., 2003. Effect of foliage spatial heterogeneity in the MODIS LAI and F_{PAR} algorithm over broadleaf forests. Rem. Sens. Environ. 85 (4), 410–423.

Slayback, D.A., Pinzon, J.E., Los, S.O., Tucker, C.J., 2003. Northern hemisphere photosynthetic trends 1982–99. Global Change Biol. 9 (1), 1–15.

Sonnentag, O., Talbot, J., Chen, J.M., Roulet, N.T., 2007. Using direct and indirect measurements of leaf area index to characterize the shrub canopy in an ombrotrophic peatland. Agric. For. Meteorol. 144 (3/4), 200–212.

Steinberg, D.C., Goetz, S.J., Hyer, E.J., 2006. Validation of MODIS F_{PAR} products in boreal forests of Alaska. IEEE Trans. Geo. Rem. Sen. 44 (7), 1818–1828.

Stenberg, P., 2007. Simple analytical formula for calculating average photon recollision probability in vegetation canopies. Rem. Sens. Environ. 109 (2), 221–224.

Stephens, B.B., Gurney, K.R., Tans, P.P., Sweeney, C., Peters, W., Bruhwiler, L., Ciais, P., Ramonet, M., Bousquet, P., Nakazawa, T., Aoki, S., Machida, T., Inoue, G., Vinnichenko, N., Lloyd, J., Jordan, A., Heimann, M., Shibistova, O., Langenfelds, R.L., Steele, L.P., Francey, R.J., Denning, A.S., 2007. Weak northern and strong tropical land carbon uptake from vertical profiles of atmospheric CO_2. Science 316 (5832), 1732–1735.

Stocks, B.J., Fosberg, M.A., Lynham, T.J., Mearns, L., Wotton, B.M., Yang, Q., Jin, J.Z., Lawrence, K., Hartley, G.R., Mason, J.A., Mckenney, D.W., 1998. Climate change and forest fire potential in Russian and Canadian boreal forests. Climatic Change 38 (1), 1–13.

Tans, P.P., Fung, I.Y., Takahashi, T., 1990. Observational constraints on the global atmospheric CO_2 budget. Science 247, 1431–1438.

Tarnavsky, E., Garrigues, S., Brown, M.E., 2008. Multiscale geostatistical analysis of AVHRR, SPOT-VGT, and MODIS global NDVI products. Rem. Sens. Environ. 112, 535–549.

Thornley, J.H.M., Cannell, M.G.R., 2004. Long-term effects of fire frequency on carbon storage and productivity of boreal forests: a modeling study. Tree Physiol. 24 (7), 765–773.

Tian, Y.H., Woodcock, C.E., Wang, Y.J., Privette, J.L., Shabanova, N.V., Zhou, L.M., Zhang, Y., Buermann, W., Dong, J.R., Veikkanen, B., Hame, T., Andersson, K., Ozdogan, M., Knyazikhin, Y., Myneni, R.B., 2002. Multiscale analysis and validation of the MODIS LAI product. ii. Sampling strategy. Rem. Sens. Environ. 83 (3), 431–441.

Turetsky, M.R., 2003. The role of bryophytes in carbon and nitrogen cycling. Bryologist 106 (3), 395–409.

Van Cleve, K., Chapin, F.S.I., Flanagan, P.W., 1986. Forest Ecosystems in the Alaskan Taiga. Springer-Verlag, New York.

van der Werf, G.R., Randerson, J.T., Giglio, L., Collatz, G.J., Kasibhatla, P.S., Arellano, A.F., 2006. Interannual variability in global biomass burning emissions from 1997 to 2004. Atmos. Chem. Phys. 6, 3423–3441.

Vogel, J.G., Gower, S.T., 1998. Carbon and nitrogen dynamics of boreal jack pine stands with and without a green alder understory. Ecosystems 1 (4), 386–400.

Wang, C.K., Bond-Lamberty, B., Gower, S.T., 2003. Carbon distribution of a well- and poorly-drained black spruce fire chronosequence. Global Change Biol. 9 (7), 1066–1079.

Welles, J.M., Norman, J.M., 1991. Instrument for independent measurements of canopy architecture. Agron. J. 83, 813–825.

White, M.A., Thornton, P.E., Running, S.W., 1997. A continental phenology model for monitoring vegetation responses to interannual climatic variability. Global Biochem. Cycles 11 (2), 217–234.

Whitehead, D., Gower, S.T., 2001. Photosynthesis and light-use efficiency by plants in a Canadian boreal forest ecosystem. Tree Physiol. 21 (12/13), 925–929.

Wu, W.L., Lynch, A.H., 2000. Response of the seasonal carbon cycle in high latitudes to climate anomalies. J. Geophys. Res. Atmos. 105 (D18), 22897–22908.

Yang, W., Shabanov, N.V., Huang, D., Wang, W., Dickinson, R.E., Nemani, R.R., Knyazikhin, Y., Myneni, R.B., 2006. Analysis of leaf area index products from combination of MODIS Terra and Aqua data. Rem. Sens. Environ. 104 (3), 297–312.

Zhang, X.Y., Friedl, M.A., Schaaf, C.B., Strahler, A.H., Hodges, J.C.F., Gao, F., Reed, B.C., Huete, A., 2003. Monitoring vegetation phenology using modis. Rem. Sens. Environ. 84 (3), 471–475.

Zhang, X.Y., Tarpley, D., Sullivan, J.T., 2007. Diverse responses of vegetation phenology to a warming climate. Geophys. Res. Lett. 34 (19), 5.

Zhou, L., Kaufmann, R.K., Tian, Y., Myneni, R.B., Tucker, C.J., 2003. Relation between interannual variations in satellite measures of northern forest greenness and climate between 1982 and 1999. J. Geophys. Res. Atmos. 108 (D1).